NEUROSCIENCE
RESEARCH ARTICLE

Eric Esquivel-Rendón et al. / Neuroscience 414 (2019) 280–296

Interleukin 6 Dependent Synaptic Plasticity in a Social Defeat-Susceptible Prefrontal Cortex Circuit

Eric Esquivel-Rendón,[a,1] Jorge Vargas-Mireles,[a,1] Roberto Cuevas-Olguín,[a] Marcela Miranda-Morales,[a] Palmira Acosta-Mares,[a] Francisco García-Oscos,[b] Juan Carlos Pineda,[c] Humberto Salgado,[c] Stefan Rose-John[d] and Marco Atzori[a,e,*]

[a] *Universidad Autónoma de San Luis Potosí, Facultad de Ciencias, San Luis Potosí, San Luis Potosí, Mexico*

[b] *Southwestern University, Department of Neuroscience, Dallas, TX, USA*

[c] *Universidad Autónoma de Yucatán, Centro de Investigaciones Regionales Hideyo Noguchi, Mérida, Yucatán, Mexico*

[d] *Christian-Albrechts Universität zu Kiel, Germany*

[e] *University of Texas at Dallas, Richardson, TX, USA*

Abstract—The role of the pro-inflammatory cytokine interleukin-6 (IL-6) in the etiology of stress-induced synaptic plasticity is yet unknown. We took advantage of a genetically modified mouse (TG) in which IL-6 trans-signaling via the soluble IL-6 receptor was blocked, to determine the role of IL-6 trans-signaling in the effects of a Social Defeat protocol (SD) on synaptic function of the medial prefrontal cortex (mPFC). Synaptic function in stress-sensitive (S) and stress-resilient (R) animals was studied in a mPFC slice preparation with whole-cell patch-clamp recording. SD altered numerous synaptic properties of the mPFC: R WT (but not TG) displayed a decreased ratio between N methyl-D-aspartate receptor (NMDAR-) dependent and amino propionic acid receptor (AMPAR-) dependent-current (I_{NMDA}/I_{AMPA}), while S WT animals (but not TG) showed a reduced ratio between AMPA and γ-amino-butyric acid receptor type A (GABA-$_A$R)-dependent currents (I_{AMPA}/I_{GABA}). Also, SD induced an increase in the frequency but a decrease in the amplitude of excitatory action-potential *dependent* PSCs (sEPSCs), both in an IL-6 dependent manner, as well as a generalized (S/R-independent) decrease in the frequency of action potential independent (miniature) excitatory (IL-6 dependent) as well as inhibitory (IL-6 independent) postsynaptic current frequency. Interestingly, corner preference (measuring the intensity of social defeat) correlated positively with I_{NMDA}/I_{AMPA} and eEPSC frequency and negatively with I_{AMPA}/I_{GABA}. Our results suggest that SD induces behaviorally-relevant synaptic rearrangement in mPFC circuits, part of which is IL-6 dependent. In particular, IL-6 is necessary to produce synaptic plasticity leading to stress resilience in some individuals, but to stress sensitivity in others.

Key words: Social defeat, IL-6, stress, GABA, synaptic inhibition/excitation ratio, NMDA/AMPA ratio.

INTRODUCTION

Genetic and environmental variables combine in unpredictable fashion, resulting in severe neuropsychiatric diseases carrying along an unbearable cost in human, social, psychological, and financial terms. Treatments for stress-related mental disease are often ineffective, costly, and plagued by hard-to-get-rid-of withdrawal and side-effects. Such dim landscape is largely associated with our scant knowledge of the etiology and cellular and molecular mechanisms underlying this wide class of conditions, many of which were fully recognized by the medical community only in the last half of the past century.

Stress may be defined as the response of an organism to a discrepancy between an acceptable or desirable state and its actual condition (Hinkle, 1987). Organisms possess large inter-individual variability in the capability to bear similar stressors (stress sensitivity and resiliency) (Selye, 1976). The role of stress in the etiology of neuropsychiatric disease has been recognized early on, particularly in clinical studies (Arnsten, 2009; Agorastos et al., 2019). In the last few decades, a series of stress-related functional alterations of the so-called *cytokine-network* has been proposed to underlie a surprisingly large number of neuropsychiatric illnesses

*Corresponding author at: Faculty of Sciences, Universidad Autónoma de San Luis Potosí, Av. Chapultepec, no. 1570, Col. Privadas del Pedregal, C.P. 78295, San Luis Potosí, San Luis Potosí, Mexico. Tel.: +52 444 826 2300x5662.
E-mail address: marco_atzori@hotmail.com (Marco Atzori).

[1] These authors contributed equally to the work.

Abbreviations: AMPA, amino propionic acid; EPSC, excitatory postsynaptic current; eXPSC, (X= E or I) evoked XPSC; GABA, g amino butyric acid; IL-6, interleukin 6; IPSC, inhibitory postsynaptic current; mPFC, medial prefrontal cortex; mXPSC, (X = E or I) miniature XPSC; NMDA, N methyl D aspartate; sgp130-GFAP, soluble glycoprotein 130 Glial Fibrillary Acidic Protein; sXPSC, (X = E or I) spontaneous XPSC; TG, transgenic; WT, wild type.

https://doi.org/10.1016/j.neuroscience.2019.07.002
0306-4522/

(Dantzer et al., 2008; Slavich and Irwin, 2014; Milenkovic et al., 2019). Particularly, increased levels of the pro-inflammatory cytokine interleukin 6 (IL-6), have positively been correlated to such diverse conditions as schizophrenic psychoses (Potvin et al., 2008), major depression (Gimeno et al., 2009; Jansen et al., 2016), bipolar disease (Jacoby et al., 2016), anxiety syndromes (Tang et al., 2018), autism spectrum syndrome (Wei et al., 2016a), but also epilepsy (Cusick et al., 2017), through yet unknown mechanisms.

In particular, increases in the serum concentration of this pleiotropic interleukin have been proposed to underlie specific behavioral phenotypes associated with different types of stress (Yang et al., 2015a) by modulating several brain areas including the infralimbic medial prefrontal cortex (mPFC) (Lin et al., 2011; Luque-García et al., 2018). Clinical observations prompted a series of animal studies indicating that IL-6, besides its systemic – prevalently immune – roles, has also the capability to directly and indirectly affect brain function (Atzori et al., 2012), is selectively elevated -together with TNF-α (another pro-inflammatory cytokine)- in major depression (Dowlati et al., 2010), is reduced by antidepressant treatment (Ramirez and Sheridan, 2016), and its serum concentration is predictive of the antidepressant efficacy of ketamine in treatment-resistant patients (Yang et al., 2015b). Molecular, immuno-histochemical, and physiological data suggest that both glial and neuronal functions are affected by the activation of the IL-6 cascade with sometimes apparently contradictory or otherwise puzzling results (Scheller et al., 2011). Among the salient effects of IL-6 reported in the central nervous system (CNS) are: neuron degeneration *and* growth (Heese, 2017), synaptic plasticity (Hernandez et al., 2016), modulation of synaptic function (Garcia-Oscos et al., 2012), modulation of transmitter release (Vezzani and Viviani, 2015), alteration of voltage-dependent membrane properties (Li et al., 2014; Xia et al., 2015), and activation and release of (other) immune factors.

In the CNS, IL-6 carries out its function mainly through the so-called trans-signaling mechanism (Rose-John, 2012; Campbell et al., 2014; Wolf et al., 2014), a mechanism through which IL-6 binds to a soluble version of the so-called IL-6 receptor (IL-6R) in the extracellular medium, binds the membrane-bound transducer glycoprotein 130 (gp130) present in all nucleated cells including neurons, and eventually activates a series of cross-phosphorylating membrane tyrosine kinases of the JAK/STAT family to produce multiple cellular and synaptic effect (Rothaug et al., 2016). In previous studies we and others have shown that IL-6 or acute stress, including administration of the bacterial toxin liposaccharide (LPS), as well as acute mild electric foot-shock, directly inhibits γ amino-butyric type A receptor ($GABA_AR$)-mediated currents (Kawasaki et al., 2008; Garcia-Oscos et al., 2012). Different from acute stress, the time scale of chronic stress has the potential to yield more profound and widespread CNS readjustments, including changes in synaptic function and plasticity and in voltage-dependent membrane mechanisms.

The purpose of this study was to determine the possible involvement of IL-6 trans-signaling in the behavioral effects of chronic stress as well as on stress-induced synaptic properties of the infralimbic prefrontal cortex, a brain area that has been implicated in the etiology of stress-related disorders (Holmes and Wellman, 2009; Moghaddam, 2016; Macht and Reagan, 2017), and with social stress in particular (Qi et al., 2018; Wang et al., 2018). We took advantage of the availability of a genetically modified mouse strain (GFAP-sgp130F_c, TG) in which IL-6 trans-signaling has been selectively inhibited in the CNS by expressing a saturating concentration of a soluble version of gp130 (sgp130F-$_c$) linked to the promoter of the astrocytic marker glial acidic fibrillary protein (GFAP) (Rothaug et al., 2016; Garbers et al., 2018). In these animals, trans-signaling was thereby blocked by a molar excess of sgp130Fc in the extracellular brain parenchyma volume, sequestrating IL-6/IL-6R complexes exclusively within the CNS (Campbell et al., 2014).

In this study we used Social Defeat (SD, a standard test of social interaction behavior)(Golden et al., 2011) as a model of chronic stress, in order to determine the possible involvement of IL-6 trans-signaling in the induction of synaptic changes induced by SD, as well as to detect possible differences in synaptic responses between susceptible (S) or resilient (R) animals (Golden et al., 2011). SD produces a psychogenic model that has been widely recognized in the rodent for the generation of a wide range of stress-induced symptoms, strongly related to the effects of chronic social diseases in humans, measuring synaptic currents in a mPFC slice preparation to determine and compare the synaptic function in WT and TG animals.

Synaptic currents in glutamatergic synapses are mediated by two main types of receptors: amino-propionic acid sensitive current (I_{AMPA}) and N-methyl D-aspartate sensitive current (I_{NMDA}). The proportion between these component is an important indicator of the maturation state of a glutamatergic synapse and of its plasticity potential (Liao et al., 1995; Wu et al., 1996; Hanse et al., 2013). On the other hand, the proportion between I_{AMPA}, and inhibitory synaptic currents mediated by γ amino butyric acid type A receptors (I_{GABA}), I_{AMPA}/I_{GABA}, is a measure of neuronal excitability (Tatti et al., 2017). Its alteration has been associated with numerous models of neuropsychiatric disease and syndromes (Lee et al., 2017; Ferguson and Gao, 2018). For these reasons here, we also investigated the possible effects of social defeat on the two ratios (I_{NMDA}/I_{AMPA} and I_{AMPA}/I_{GABA}) along with other indicators of synaptic function.

EXPERIMENTAL PROCEDURES

Experimental animals

We used 135 male mice, 67 wild type (C57BL/6J, Charles River, WT), and other 68 of the same strain, offspring from mice genetically modified in the laboratory of SRJ (GFAP-gp130Fc, TG). Animals were housed in a facility at room temperature (23 °C), with an inverted light cycle (light between 7 PM and 7 AM, dark from 7 AM to 7 PM) and fed with standard rodent diet (chow 5001, Nutrimix, Mexico City). All animals used, in the age range between 10 and 22 weeks old, were housed individually for at least the last 10 days before starting the protocol, and tested and/or sacrificed for electrophysiological experiments between 10 AM and 1 PM.

GFAP-sgp130Fc animals

A transgenic mouse expressing sgp130Fc in the central nervous system by astrocytes (GFAP-sgp130Fc mice) was previously described (Campbell et al., 2014). A vector containing the human glial fibrillary acidic protein GFAP promoter cloned upstream of the optimized soluble glycoprotein 130Fc (sgp130Fc) (Campbell et al., 2014) was used for the construction of the transgenic mice expressing sgp130Fc in the central nervous system by astrocytes (GFAP-sgp130Fc mice, TG); a Bcl II/Not I fragment of 5854 bp was isolated from the plasmid and injected into oocytes, which were implanted into foster mothers. The following primers were used for genotyping sgp130Fc mice:

sgp130-Fc-screen forward: 5′-GAG TTC AGA TCC TGC GAC-3′.
sgp130-Fc-screen reverse: 5′-TCA CTT GCC AGG AGA CAG-3′.

Social Defeat protocol

In brief, the SD protocol consists in a 10-min per day interaction of a novel (never presented before) experimental animal (WT or TG) with a different CD1 albino mouse every day during a 10-day period (Golden et al., 2011). CD1 mice were pre-selected by age (between 6 and 8 weeks old) and by aggressiveness (only those who seize an intruder at least twice for longer than 30 s in a 3-min time). Aggressive physical contact was stopped by the experimenter before physical injury or wounding to either animal could actually occur, typically after 5–10 min of interaction. The C57BL/6 and CD1 mice were subsequently separated by a transparent Plexiglas wall set across the long half of a rectangular cage of size 20 × 50 × 15 (width × depth × height) cm with a dozen holes (about 1 cm in diameter) for the remainder of the 24-h period as described in previous studies (Golden et al., 2011).

Determination of stress sensitivity

The sensitivity to stress was determined using the same experimental protocol used in Golden et al. (2011). In brief, we measured the time spent in the interaction zone with a CD1 (TIZ), in the presence or in the absence of a CD1 mouse enclosed in an 8 × 6 × 30-cm (width × depth × height) cage in the center of the edge of a set up sized 42 × 42 × 40 cm (width × depth × height) during 150 s, as well as the Time spent by the experimental animal in the Corner Areas (TCA) in the presence of the CD1 in the enclosure:

$$SIR = \frac{\text{Time in Interaction Zone in } \mathbf{presence} \text{ of a CD1}}{\text{Time in Interaction Zone in } \mathbf{absence} \text{ of a CD1}}$$

or

$$SIR = \frac{\text{TIZ(w/CD1)}}{\text{TIZ(w/o CD1)}}$$

In agreement to a previous studies (Golden et al., 2011), we defined as sensitive (S) animals those whose Social Interaction Ratio (SIR) was <1, and as resilient (R) those animals whose SIR was ≥1. For each experimental animal we also measured the Corner Preference Index (CPI) defined as:

$$CPI = \frac{\text{Time in Corner Area}}{\text{Time in Corner Area} + \text{Time in Interaction Zone}}$$

or

$$CPI = \frac{\text{TCA}}{\text{TCA} + \text{TIZ}}$$

All behavioral experiments were video recorded for post-hoc visual analysis by a previously trained observer for extraction of behavioral parameters.

Other behavioral tests

Sucrose preference index

Animals were housed individually with the availability of two bottles, one with standard, purified water, and a second one with the same liquid but with 10% sucrose. Sucrose preference was determined as the ratio between the volume of sweet water drunk divided by total water ($V_{tot} = V_{sweetened} + V_{normal}$) ingested:

$$\text{SPI} = \text{V}_{\text{sweetened}}/(\text{V}_{\text{sweetened}} + \text{V}_{\text{normal}})$$

Porsolt forced swimming

Animals were gently put in a 2-L beaker containing 1.5 L water at 23 °C. We measured the latency to immobility starting at the moment of immersion, and total immobility time during the last 4 of the 6-min immersion. All behavioral experiments were video recorded for post-hoc analysis.

Electrophysiological experiments

Experimental animals were either subject to a protocol of Social Defeat (SD), as described in previous work (Golden et al., 2011), or not subject to such protocol (control, CT). After the behavioral response of experimental animals was evaluated (within the 3 days following the end of the SD protocol), animals were used the next day for electrophysiological recording.

Brain slices

Similar to previous work (Roychowdhury et al., 2014), mice were anesthetized with isoflurane (Baxter, Round Lake IL), and sacrificed according to the NIH and Norma Nacional Mexicana rules (UASLP protocol no. 2240) and their brains sliced with a vibrotome (VT1000, Leica) in a cold solution (0–4 °C) containing (mM) 126 NaCl, 3.5 KCl, 10 glucose, 25 $NaHCO_3$, 1.25 NaH_2PO_4, 1.5 $CaCl_2$, 1.5 $MgCl_2$, at pH 7.4 and saturated with a mixture of 95% O_2 and 5% CO_2 (ACSF). Coronal slices 270 μm thick were taken from the infralimbic medial prefrontal cortex and incubated in ACSF at 32 °C before being placed in the recording chamber. Once in the recording chamber, neurons were selected by their pyramidal shape and by their pronounced apical

dendrite, suggestive of pyramidal cell morphology, using an upright microscope (BX51, Olympus, Japan) with a 60× objective and an infrared camera system (DAGE-MTI, Michigan City, IN). Whole-cell voltage-clamp recordings from layer V pyramidal neurons of the medial prefrontal cortex (mPFC) were performed under visual guidance.

Drugs, solutions, and electrophysiological recordings

Electrically evoked excitatory or inhibitory postsynaptic potentials (eEPSCs or eIPSCs) were elicited by delivering two electric stimuli (100–200 μs, 10–50 μA) 100 ms apart, every 15 s, through a glass stimulation monopolar electrode filled with ACSF at about 100–200 μm from the recorded neuron located in layer II/III, dorsal to recording cell somata. The holding voltage was corrected for the junction potential (V_{offset} < 9 mV). All intracellular recording solutions were titrated around pH 7.3, and had an osmolarity of approximately 270 mOsm.

eEPSCs and eIPSCs were monitored at different stimulation intensities prior to baseline recording. Detection for both electrically-evoked and spontaneous synaptic currents threshold was set at ≈150% of one standard deviation of the noise (typical noise ≈4–5 pA, threshold ≈7–8 pA). A 2-mV 100-ms-long voltage pulse was applied at the beginning of every episode and access resistance (10–20 MΩ) was monitored throughout the experiment in order to evaluate the quality of the recordings. Recordings displaying >20% change in input or access resistance were discarded from the analysis. All signals were filtered with a low-pass Butterworth filter at 2 kHz and sampled at 10 kHz. Experiments were performed at room temperature (22–23 °C).

6,7-Dinitroquinoxaline-2,3-dione (DNQX, 10 μM), and kynurenate (2 mM), or bicuculline methiodide (10 μM) were used for blocking α-amino-3-hydroxy-5-methyl-4-isoxazole-propionic acid receptor (AMPAR)-, N-methyl-D-aspartate receptor (NMDAR)-mediated currents, or γ-amino-butyric acid type A receptor- ($GABA_A$R) mediated currents, respectively. More details are available in previous work (Garcia-Oscos et al., 2012).

Input–output curves

Input/output (I/O) curves were recorded with 3–5-MΩ electrodes filled with a solution containing (mM): 100 CsCl, 5 1,2-bis(2-aminophenoxy)ethane-N,N,N′,N′-tetraacetic acid K (BAPTA-K), 1 lidocaine N-ethyl bromide (QX314), 1 $MgCl_2$, 10 N-(2-hydroxyethyl) piperazine-N′-(2-ethanesulfonic acid) (HEPES), 4 glutathione, 1.5 ATPMg, 0.3 $GTPNa_2$, 20 phosphocreatine at a holding membrane potential V_h = −60 mV. The amplitude of electrically evoked (e)IPSCs was quantified as mean peak amplitude of 4–10 pulses at increasing stimulation intensities until the mean response reached a plateau or, sometimes, showed a decreased response for stronger stimulation intensities, as previously reported (Garcia-Oscos et al., 2014).

Measurement of I_{AMPA}/I_{GABA}

We measured inhibitory and excitatory currents within the same neuron, using a low-Cl^- intracellular solution containing where CsCl was lowered from 100 to 10 mM, and the remainder 90 mM was substituted with K-gluconate, eliciting a theoretical reversal potential for Cl^- of approximately −63 mV. Similar to previous work (Garcia-Oscos et al., 2012), reversal potential for both glutamatergic and GABAergic postsynaptic currents was evaluated determining current–voltage (I-V) relationships, for the evoked post synaptic current (peak amplitude of 10 events at each holding potential V_h in the range from V_h = −90 mV up to V_h = +60 mV). Evoked IPSCs reversed polarity close to the theoretical reversal potential of −63 mV (−64 ± 2 mV, n = 3), which was used as a holding potential for recording glutamatergic currents (I_{AMPA}), while evoked EPSCs reversed at V_{exc} = 30.5 ± 3 mV (n = 3), whereby V_h = +30 mV was used as a holding potential for recording GABAergic currents (I_{GABA}, data not shown). The nature of I_{AMPA} and I_{GABA} was confirmed by blocking them as specified above, the former with a mixture of kynurenic acid (2 mM) and DNQX (10 μM), and the latter with 10 μM bicuculline methiodide (data not shown).

Measurement of I_{NMDA}/I_{AMPA}

We also used patch-clamp recording for measuring the ratio between N-methyl-D-aspartate-receptor-mediated currents (I_{NMDA}) and alpha-amino-3-hydroxy-5-methyl-4-isoxazole-propionic-acid-receptor-mediated currents (I_{AMPA}) from pyramidal neurons like in previous work (Dufour et al., 2006). In this case, the control solution contained bicuculline methiodide (10 μM) for blocking, γ-aminobutyric-acid A-receptor ($GABA_A$R)-mediated currents. Postsynaptic currents were recorded with 3–5-MΩ electrodes using a solution containing the following (in mM): 100 CsOH, 100 gluconic acid, 5 1,2-bis(2-aminophenoxy) ethane-N, N,N′,N′-tetraacetic acid K (BAPTA-K), 1 lidocaine N-ethyl bromide (QX314), 1 $MgCl_2$, 10 N-(2-hydroxyethyl)piperazineN′-(2-ethanesulfonic acid) (HEPES), 4 glutathione, 1.5 $ATPMg_2$, 0.3 $GTPNa_2$, 8 biocytin. As shown in Fig. 2, I_{AMPA} were recorded at a holding potential V_r = −60 mV and measured at their peak. I_{NMDA} were recorded in the same cell at V_r = +60 mV in order to fully remove the Mg^{2+} block at NMDA receptors. I_{NMDA} amplitude was calculated as the mean between 95 and 105 ms after the electric stimulation, for minimizing the possible contamination by I_{AMPA}.

Spontaneous and miniature synaptic currents

Glutamatergic and GABAergic spontaneous postsynaptic currents (sEPSCs and sIPSCs, respectively) were recorded in the same conditions described for their electrically evoked counterparts (eEPSCs and eIPSCs). Miniature EPSCs and IPSCs (mEPSCs and mIPSCs) were recorded in the same conditions but in the presence of the Na^+-current blocker tetrodotoxin (TTX, 1 μM, Alomone Labs., Israel). Synaptic event amplitude and frequency were measured by using the MiniAnalysis program (Synaptosoft, Fort Lee, NJ, USA) with samples of 200–1000 events each. 20–80% rise-time (rt) and half-width time (hw, time width of the event at 50% amplitude) were calculated as the averages from 10 or more synaptic events selected in a similar

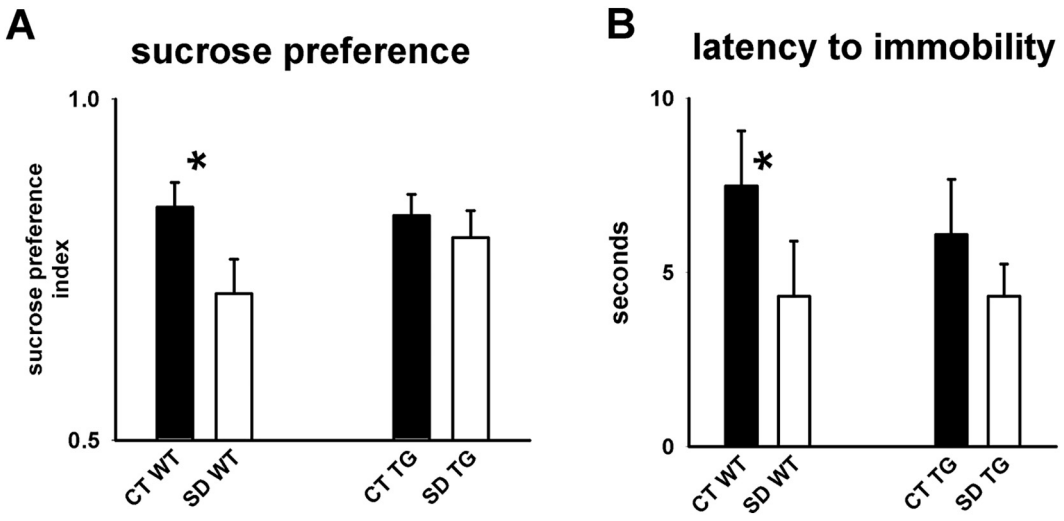

Fig. 1. Behavioral response to SD. (A) Sucrose preference is significantly decreased by SD in WT animals (bars on the left) but not in TG animals (bars on the right). **(B) Latency to immobility** in the Porsolt forced swim test is significantly decreased in WT animals but not in TG ones. This results indicate that SD was overall effective in the induction of stress, and that IL-6 trans-signaling is involved in the effect.

amplitude range, in order to avoid bias due to amplitude dependence.

Statistical analysis

χ^2 tests were used to assess differences between behavioral parameters. Synaptic parameters between experimental groups were compared using 2 × 2 ANOVA for WT vs. TG and unstressed vs. stressed (pooling together S and R animals), whereas a 2 × 3 ANOVA was used to compare WT vs. TG and control (unstressed) and, separately, the two stressed (S, and R) groups. Sample size was the number of recording from each group ($9 \leq n \leq 28$ recordings for each statistic, except one (1/28) statistic with seven recordings; at least three animals per group for each set of recordings, as indicated in the corresponding figure). Sample size is indicated in the respective figure legend, for all data shown in the figures, or in the text, otherwise. Results of ANOVA F test are reported only for statistically significant differences. Those groups whose statistical significance was assessed by the ANOVA F value were further analyzed using as Tukey HSD. Calculation of synaptic parameters was based on measurement using statistically stable means, defined as means averaged on statistically stable periods. A statistically stable period is defined as a time interval (5–8 min) along which postsynaptic current mean amplitude measured during any 2-min assessment did not vary according to Mann–Whitney U test. All data are expressed as mean ± S.E.M. Pair pulse ratios (PPR) were calculated as means of the second response divided by the mean of the first response, according to Kim and Alger (2001). Data were reported as different only if $p < 0.05$. Single, double, or triple asterisks (*, **, ***) indicate $p < 0.05$, 0.02, or 0.01, respectively. Pound sign (#) indicates statistical tendency ($p < 0.10$). Whenever sample size is not reported in the text it is shown in the corresponding figure.

RESULTS

Behavior

SD increased the overall percentage of susceptible animals (SIR < 1) from 11.9% (8/67) to 26.5 (18/68) ($\chi^2 = 6.95$, df = 1, $p < 0.01$). Interestingly, while 18.2% (6/33) control (not previously subject to SD, CT) WT animals were classified as S, only 5.9% (2/34) of the TG CT animals turned out to be sensitive ($\chi^2 = 7.14$, df = 1, $p < 0.01$). On the other hand, WT and TG displayed similar proportions of S mice (29.4%, 10/34), and (23.5%, 8/34), respectively, suggesting that inhibition of IL-6 trans-signaling does *not* prevent SD-induced behavior ($\chi^2 = 0.89$, df = 1, $p = 0.34$). Direct two-way ANOVA of the SIR parameter showed that the SD was effective in producing stress ($F_{1,134} = 31.7$, $p < 0.01$) regardless of animal group (WT vs. TG, $F_{1,134} = 0.29$, n.s.).

Social Defeat stresses C57BL/6 mice in a IL-6-dependent manner

We assessed the effectiveness of SD and its IL-6 dependence by measuring anhedonia (Sucrose Preference Index, SPI) and latency to immobility (LTI) in the four experimental groups (WT unstressed, WT subject to SD, TG unstressed, and TG subject to SD, Fig. 1). Two-by-two ANOVA indicated significant differences in both tests ($F = 5.76$, $p < 0.02$, df = 131 for sucrose preference test; $F = 3.94$, $p < 0.05$, df = 134 for time to immobility in Porsolt forced swimming test). Post-hoc Tukey test showed that while WT/SD animals displayed decreased SPI compared to WT/unstressed (Fig. 1A: 0.84 ± 0.04 for WT/unstressed vs.0.71 ± 0.05 for WT/SD, n = 34 $p < 0.01$), on the contrary, TG animals did not show any SD-caused difference in SPI (0.83 ± 0.03 in TG/unstressed, n = 34, vs. 0.80 ± 0.04 in TG/SD, n = 34, n.s.). Similarly, latency to immobility in the Porsolt forced-swimming test was

decreased by SD in WT (LTI = 7.5 ± 1.6 in WT/unstressed, n = 33, vs. 4.3 ± 1.6 in WT/SD, n = 31, $p < 0.01$) but not in TG animals (Fig. 1B: LTI = 6.1 ± 1.6 in TG/unstressed, n = 33, vs. 4.3 ± 0.9 in TG/SD, n = 34, n.s.). These data suggest that SD is an effective stressor in WT animals, and that IL-6 trans-signaling is involved in its behavioral stressing effects.

Synaptic changes induced by SD

We used patch-clamp recording in the output layer (layer 5) from the infralimbic mPFC to determine possible synaptic changes induced by SD in the mPFC network. Mean input resistance, measured for each recording with a 5-mV negative voltage pulse delivered before each electric stimulation was in the range 104–453 MΩ. No differences in input

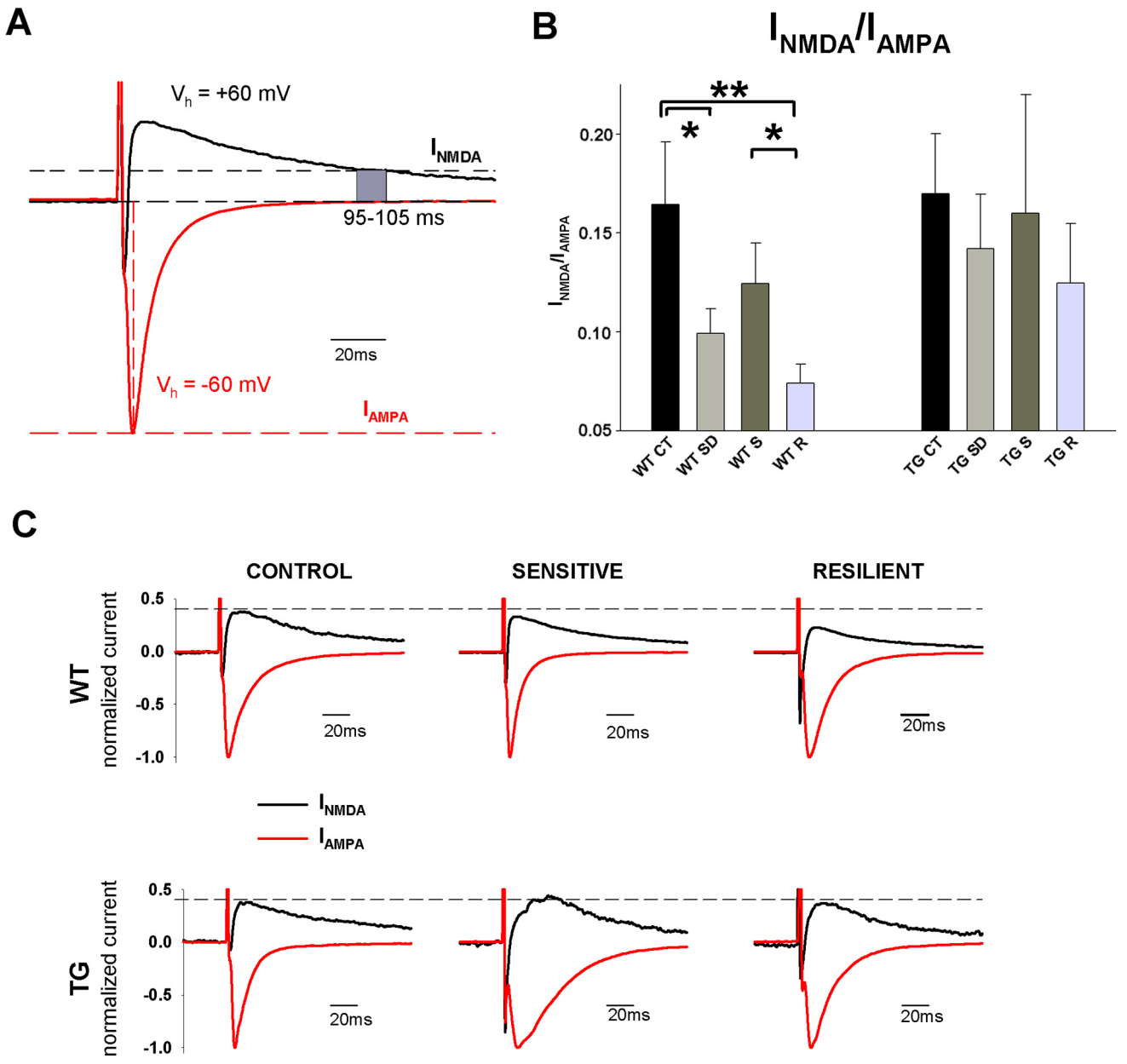

Fig. 2. SD decreases the ratio I_{NMDA}/I_{AMPA} in resilient animals. (A) NMDAR-mediated currents (I_{NMDA}) were measured as the mean current between 95 and 105 ms, for avoiding contamination by faster kinetic AMPA component, at a holding current of V_h = +60 mV, after the delivery of the electric stimulation (gray area). AMPAR-mediated currents (I_{AMPA}) were measured as peak current at V_h = −60 mV (red trace). **(B)** First four bars on the left refer to WT animals, last four bars on the right represent the results from TG. CT: control (unstressed animals), SD: pool of the SD-stressed recorded animals, S: SD-Susceptible animals, R: SD-Resilient animals. Same bar legend for Figs. 2–4. Compared to unstressed animals I_{NMDA}/I_{AMPA} is significantly reduced in the whole pool of stressed animals and in resilient animals but not in sensitive animals. The effect is not present in TG animals (bars on the right). Sample size, from left to right bars: n = 10 for WT CT, 20 WT pool, 10 WT S, 10 WT R; TG: CT: 20, TG pool: 10, TG S, 10 TG R. **(C) Representative recordings** from unstressed (left: CONTROL), SD-sensitive (center: SENSITIVE), and SD-resilient (right: RESILIENT) WT (above) and TG (below) animals. NMDA currents are shown in black (top trace of each graph), while AMPA currents are shown in red (lower trace of each graph).

resistance were revealed by 2 × 2 ANOVA analysis of WT vs. TG and unstressed vs. SD animals (unstressed WT: 287 ± 29 MΩ, n = 16; unstressed TG: 387 ± 60 MΩ, n = 20; SD WT: 305 ± 25 MΩ, n = 20; SD TG: 270 ± 24, n = 20), or by a 3 × 2 ANOVA of WT vs. TG and unstressed, Sensitive, and Resilient animals (WT S: 299 ± 42 MΩ, n = 10; WT R: 313 ± 29, n = 10; TG S: 274 ± 46 MΩ, n = 10; TG R: 266 ± 20 MΩ, n = 10), suggesting no gross differences in passive cell properties between any groups.

In all bar graphs in Figs. 2–5 we show the results for different synaptic parameters measured in the study. In all these figures, the first group of four bars represents the mean ± s.e.m. from WT animals in the following order: 1) control (CT, no SD), 2) the whole pool of recorded SD animals (SD), 3) susceptible animals (S), and 4 resilient animals (R). The second group of bars (5th to 8th) represents the results of the same group of experiments as in bars 1–4, but for the TG group. The significant results of statistics are reported in the text.

SD selectively decreases I_{NMDA}/I_{AMPA} in resilient animals in an IL-6 dependent manner

The ratio between different glutamatergic components is a critical indicator of the plastic state of excitatory synapses (Thomas et al., 2001; Moga et al., 2006). For this reason, we measured the ratio between the NMDAR-dependent and the AMPAR-dependent components of the synaptic glutamatergic currents (I_{NMDA}/I_{AMPA}) evoked by stimulation of adjacent layer 2/3, by first recording I_{AMPA} at hyperpolarized potentials V_r = −63 mV (at which I_{NMDA} is minimized by Mg^{+2} block), and then depolarizing the neuron at a resting potential V_r = +60 mV in order to fully release Mg^{+2} block of I_{NMDA}. I_{NMDA} was measured as the mean between 95

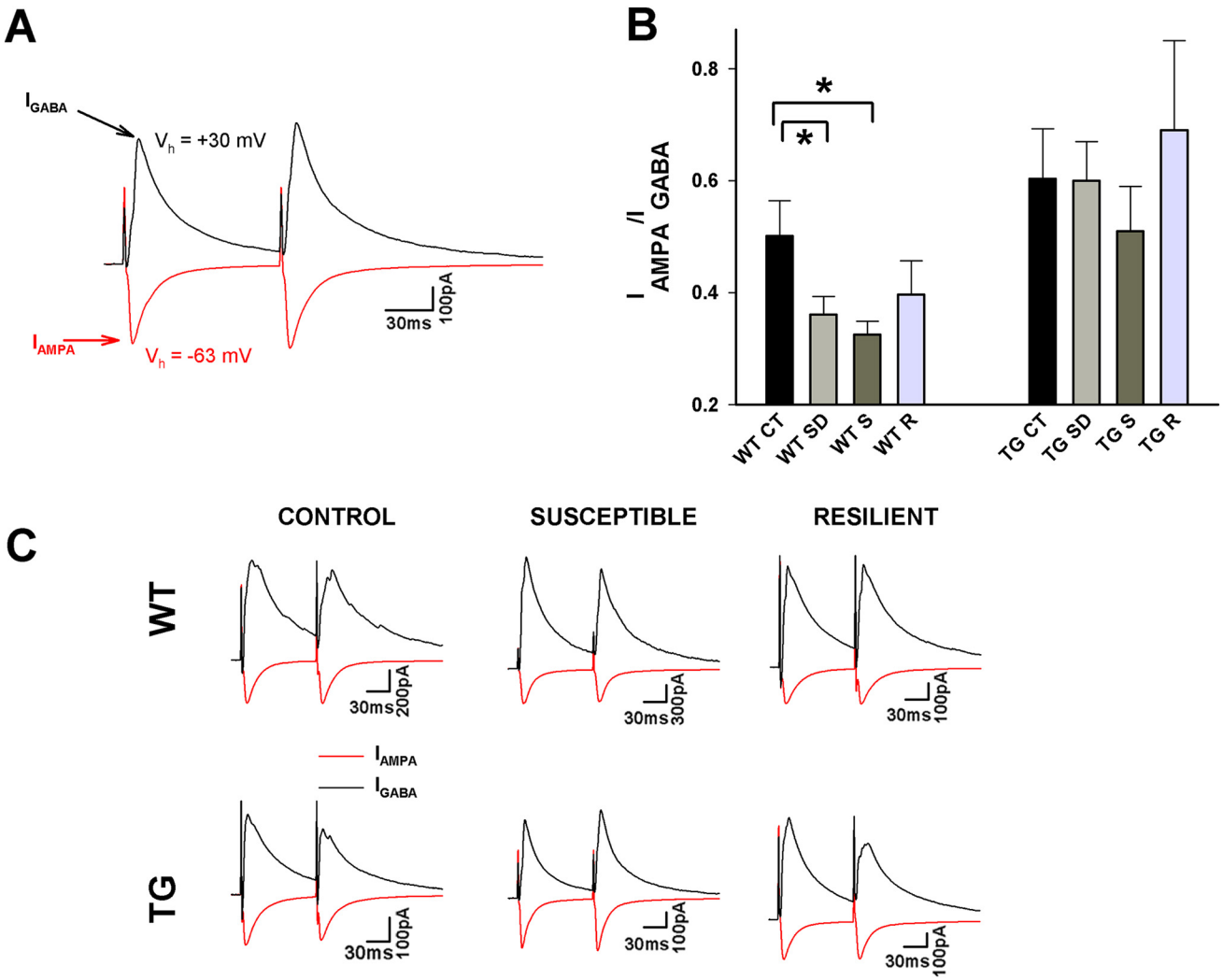

Fig. 3. SD decreases the ratio I_{AMPA}/I_{GABA} in sensitive animal. (A) I_{GABA} and I_{AMPA} were measured respectively at a holding potential of V_h = −63 mV and V_h = +30 mV, respectively, as peak amplitude (upper black trace and lower, red trace, respectively). **(B) SD significantly decreases I_{AMPA}/I_{GABA}** specifically in sensitive animals, but not in R ones (same bar legend as in Fig. 1B). The effect is not present in TG animals (bars on the right). Bar legend as above. Sample size, from left to right bars: n = 16 for WT CT, 20 WT pool, 10 WT S, 10 WT R; 9 TG CT, 20 TG pool, 10 TG S, 10 TG R. **(C) Representative recordings of I_{AMPA} and I_{GABA}** for WT (above) and TG (below) for unstressed animals (left: CONTROL), stress-susceptible (center: SENSITIVE), and resilient (right, RESILIENT).

and 105 ms after the onset of the stimulating pulse in order to eliminate I_{AMPA} contamination (Fig. 2A, see the *Materials and Methods* section for details).

In WT animals, I_{NMDA}/I_{AMPA} of the overall SD pool was significantly reduced compared to unstressed animals (two-by-two ANOVA $F_{1,59} = 5.51$, $p < 0.02$, *post-hoc* Tukey test, $p < 0.01$). Three-by-two ANOVA showed an SD effect ($F_{1,59} = 4.51$, $p < 0.02$, n = 10 each group). Post-hoc analysis indicated that resilient (R) animals possessed a lower I_{NMDA}/I_{AMPA} compared to both CT (Tukey test, $p < 0.01$) and S animals (Tukey test, $p < 0.05$), suggesting a resilient-specific mPFC plasticity (Fig. 2B, bars on the left). Interestingly, the reduction was absent in TG animals, indicative of an IL-6 trans-signaling dependence (Fig. 2B, bars on the right). Representative recordings of I_{NMDA} and I_{AMPA} normalized to I_{AMPA} are shown in Fig. 2C for in WT and TG animals from unstressed, stress-resilient, and stress-sensitive animals, as indicated in the figure.

SD selectively decreases I_{AMPA}/I_{GABA} in resilient animals in an IL-6 dependent manner

The ratio I_{AMPA}/I_{GABA} is an estimation of synaptic neuronal excitability (Maffei et al., 2004). Analogous to the ratio I_{NMDA}/I_{AMPA}

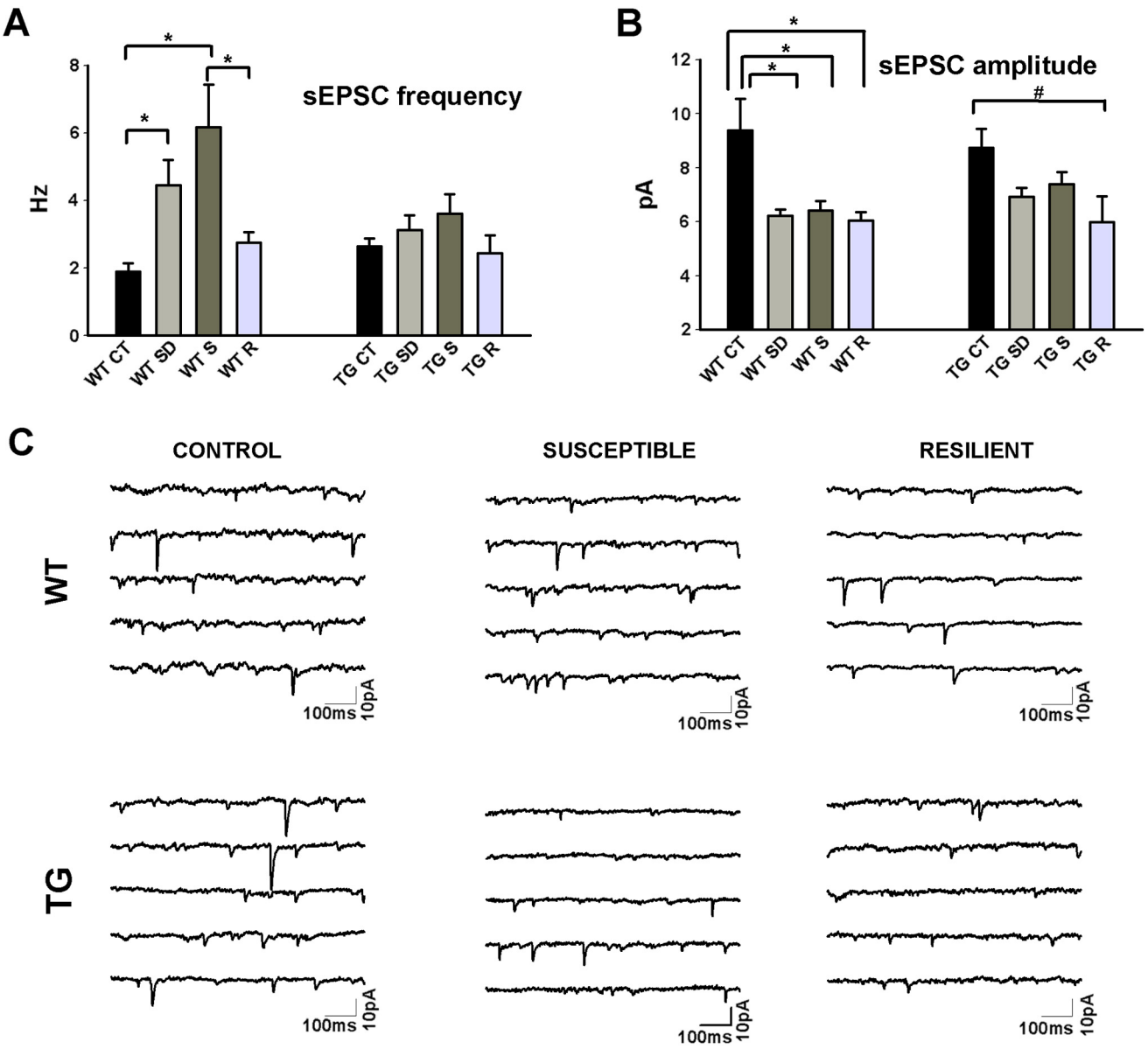

Fig. 4. Effect of SD on action-potential dependent glutamatergic spontaneous release. (A) The frequency of action-potential dependent spontaneous excitatory currents (sEPSCs) in the pool of WT SD animals, particularly in S (but not R) animals is higher than in unstressed animals. This effect is absent in TG animals. **(B) The amplitude of sEPSCs** is decreased by SD. The decrease is present both in S and R WT animals (bars on the left) but is absent in TG animals (bars on the right). Bar legend as above. Sample size, from left to right bars: n = 9 for WT CT, 20 WT pool, 10 WT S, 10 WT R; 10 TG CT, 20 TG pool, 10 TG S, 10 TG R. Fig. 3C**: Representative sEPSC traces** in control (unstressed, left), and in SD-susceptible (center) or SD-resilient (right) animals, for WT (upper traces) and TC (lower traces animals).

we measured I_{AMPA}/I_{GABA} by first recording the amplitude of excitatory I_{AMPA} at the hyperpolarized potential $V_r = -63$ mV corresponding to the reversal potential for I_{GABA}, and then measuring I_{GABA} at the reversal potential for I_{AMPA}, $V_r = +30$ mV in the same recorded neuron for all the neurons of each group (Fig. 3A, for details see the *Materials and Methods* section).

Two-by-two ANOVA suggested that SD significantly reduces I_{AMPA}/I_{GABA} ratio in WT mice ($F_{1,64} = 4.1$, $p < 0.05$). Post-hoc Tukey test shows that the pool of SD WT (but not TG) animals has a lower I_{AMPA}/I_{GABA} ratio compared to both unstressed animals ($p < 0.05$). Three-by-two ANOVA (WT vs. TG, and CT, S, and R) suggests that the mean of the SD groups deviates from the average. Post-hoc analysis showed that I_{AMPA}/I_{GABA} in unstressed WT animals is significantly decreased selectively in S (Fig. 3, third bar, Tukey test, $p < 0.05$) but not in R mice (fourth bar). Such effect was absent in TG animals (Fig. 3B, right). We also analyzed separately the effect of SD on pair pulse ratio (PPR) on both excitatory and inhibitory evoked transmission. No significant differences were found between control (non-stressed) and SD animals in either excitatory or inhibitory synaptic transmission (n = 9 for WT CT, n = 10 all other groups, data not shown). Representative recordings of I_{GABA} and I_{AMPA} in WT and TG animals are shown Fig. 3C for unstressed, stress-resilient, and stress-sensitive animals, as indicated in the figure.

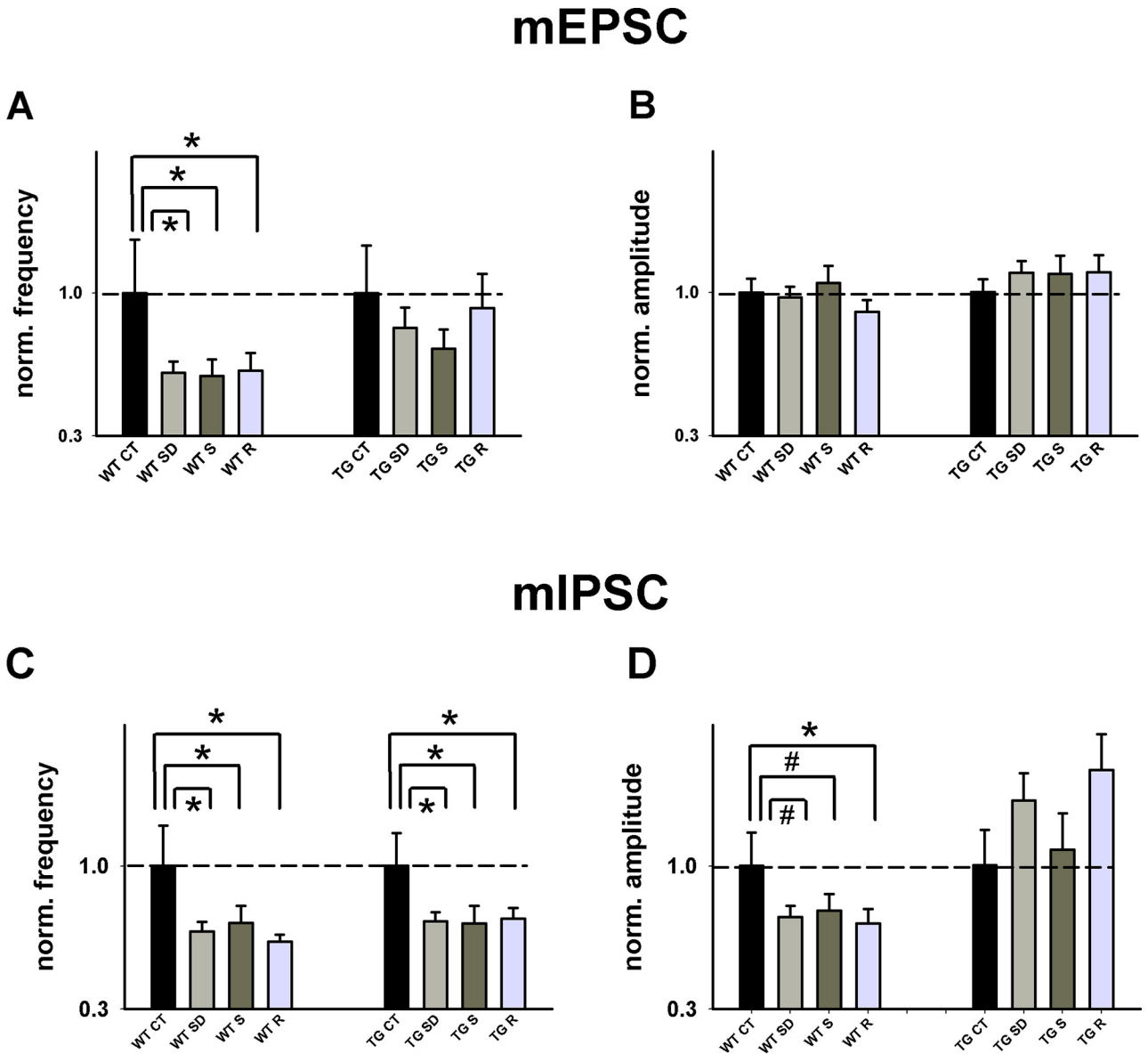

Fig. 5. Effect of SD on action potential-independent transmission. (A) SD decreases **mEPSC frequency in** WT animals leaving it unchanged TG animals. **(B)** SD did not change mEPSC amplitude. Two-by-two ANOVA $p < 0.05$). This effect is absent in TG animals. Bar legend as above. Sample size, from left to right bars: n = 11 for WT CT, 26 WT pool, 13 WT S, 13 WT R; 11 TG CT, 23 TG pool, 11 TG S, 12 TG R. **(C)** SD decreases mIPSC frequency (first four bars) in WT and TG animals (last four bars). **(D)** mIPSC amplitude shows a trend for decreased amplitude (first four bars), in WT (left bars) but not in TG animals (right bars). Bar legend as above. Sample size, from left to right bars: n = 10 for WT CT, 28 WT pool, 15 WT S, 13 WT R; 9 TG CT, 21 TG pool, 11 TG S, 10 TG R.

The decrease in excitability may be caused – at least in part – by an increase in inhibition in stress-susceptible animals, as also reported in previous work (McKlveen et al., 2016), in agreement with an increased saturation of inhibitory currents (I_{GABA}) input–output (I/O) curves from electrically evoked (e)IPSCs detected in WT S animals (+123 ± 59%, n = 5 and 10 for CT and S animals, respectively, $p < 0.05$) but not in TG animals (+30 ± 29%, n = 5 and 10 for CT and S animals, respectively, n.s.).

Stress sensitivity induces an IL-6-dependent increase in spike-dependent excitatory activity

Both excitatory and inhibitory spontaneous post-synaptic currents (sEPSCs and sIPSCs) were recorded in order to detect possible effects of SD on action-potential *dependent* synaptic activity. Two-by-two ANOVA of sEPSCs suggested a significant effect of SD on both sEPSCs frequency ($F_{1,58} = 30.55$, $p < 0.01$) and amplitude ($F_{1,58} = 20.65$, $p < 0.01$) (Fig. 4A). Post-hoc Tukey test showed that SD increased sEPSC frequency ($p < 0.01$, Fig. 3A) and reduced the amplitude ($p < 0.01$, Fig. 4B) in WT but not in TG animals. Two-by-three ANOVA was significant for an effect of SD ($F_{columns} = 9.29$, $p < 0.001$). Post hoc Tukey test indicated that sEPSC frequency increased about threefold selectively in S ($p < 0.01$) but not in R WT animals (Fig. 4A). The effect was absent in TG animals.

sEPSC amplitude was significantly reduced in both in S and R (SD) animals ($p < 0.01$ both), also in an IL-6 dependent fashion, although R animals displayed a tendency to a reduced amplitude. Representative recordings are shown in Fig. 3C for unstressed (control, left), stress-susceptible (center), and stress-resilient (right) WT mice (above), and TG mice (below). No SD-induced effects, in amplitude or in frequency, were detected in sIPSCs (n = 9 for WT CT, n = 10 for all other groups, data not shown).

SD induces a reduction in the frequency of miniature events

In order to determine a more specific effect of SD on synaptic function we measured the frequency, amplitude, and kinetics of pharmacologically isolated miniature excitatory and inhibitory postsynaptic currents (mEPSCs and mIPSC, respectively) in the presence of the Na^{2+}-channel blocker tetrodotoxin (TTX, 1 μM).

Two-by-two ANOVA indicated an effect of SD on mEPSC frequency ($F_{columns} = 4.5$, $p < 0.05$). Two-by-three ANOVA suggested that both S and R mice display a lower mEPSC *frequency* (Fig. 5A), compared to unstressed animals ($F_{columns} = 6.35$, $p < 0.02$). Post hoc Tukey test indicated that both stressed groups displayed lower sEPSC frequency compared to unstressed mice (either S or R vs. unstressed: $p < 0.01$) in WT but not in TG animals. SD did not significantly change mEPSC *amplitude* in WT or in TG animals (Fig. 5B). These changes suggest IL-6 trans-signaling pathway affects presynaptic glutamate release, besides other possible effects.

Similar to mEPSC, SD also decreased mIPSC *frequency* both in S and R animals, but, contrary to mEPSC, the reduction was present both in WT as well as in TG mice (Figs.5C), indicating that IL-6 trans-signaling is not involved in this particular effect. In fact, both two-by-two ANOVA and two-by-three ANOVA showed an overall effect of stress on mIPSC frequency ($F_{columns} = 9.29$, $p < 0.01$, and $F_{columns} = 9.93$, $p < 0.001$, respectively). Post-hoc Tukey test indicated that both S and R mice displayed lower sIPSC frequency both in WT (unstressed vs S, and unstressed vs. R, $p < 0.01$

Table 1. . SD-induced change in synaptic parameters. Arrow up () or down (¯) ind(icate statistically significant increase or decrease, respectively. IL-6 dependence indicates whether a similar change occurred or not in a similar experiment in GFAP-sgp130Fc TG animals. We report different behavior between S and R groups either because S differs from control while R does not or vice versa *and/or* there is a direct difference between the S and R group means. It is worthwhile noticing that while the parameter values of R and S animals may or may not differ from each other, regardless of their behavior with respect to control (unstressed) animals, and vice-versa, due to statistical error. The pound symbol (#) indicates statistical tendency ($p < 0.10$).

parameter	change in stress-Sensitive animals	IL-6 dependent?	change in stress-resilient animals	IL-6 dependent?	different behavior between R and S	IL-6 dependent?
glutamate synapses I_{NMDA}/I_{AMPA} component ratio	0	–	↓	yes	yes	yes
excitatory/inhibitory synaptic ratio I_{AMPA}/I_{GABA}	↓	yes	0	–	yes	yes
Paired pulse ratio (PPR) glutamate	0	–	0	–	no	–
Paired pulse ratio (PPR) GABA	0	–	0	–	no	–
sEPSC frequency	↑	yes	0	–	yes	yes
sEPSC amplitude	↓	yes	↓	0 (#)	no	–
sIPSC frequency	0	–	0	–	no	–
sIPSC amplitude	0	–	0	–	no	–
mEPSC frequency	↓	yes	↓	yes	no	–
mEPSC amplitude	0	–	0	–	no	–
mIPSC frequency	↓	no	↓	no	no	–
mIPSC amplitude	0 (#)	–	↓	yes	no	–
mEPSC rise time	0	–	0	–	no	–
mIPSC rise time	0	–	0	–	no	–
mEPSC half width	0	–	0	–	no	–
mIPSC half width	0	–	↑	yes	yes	–

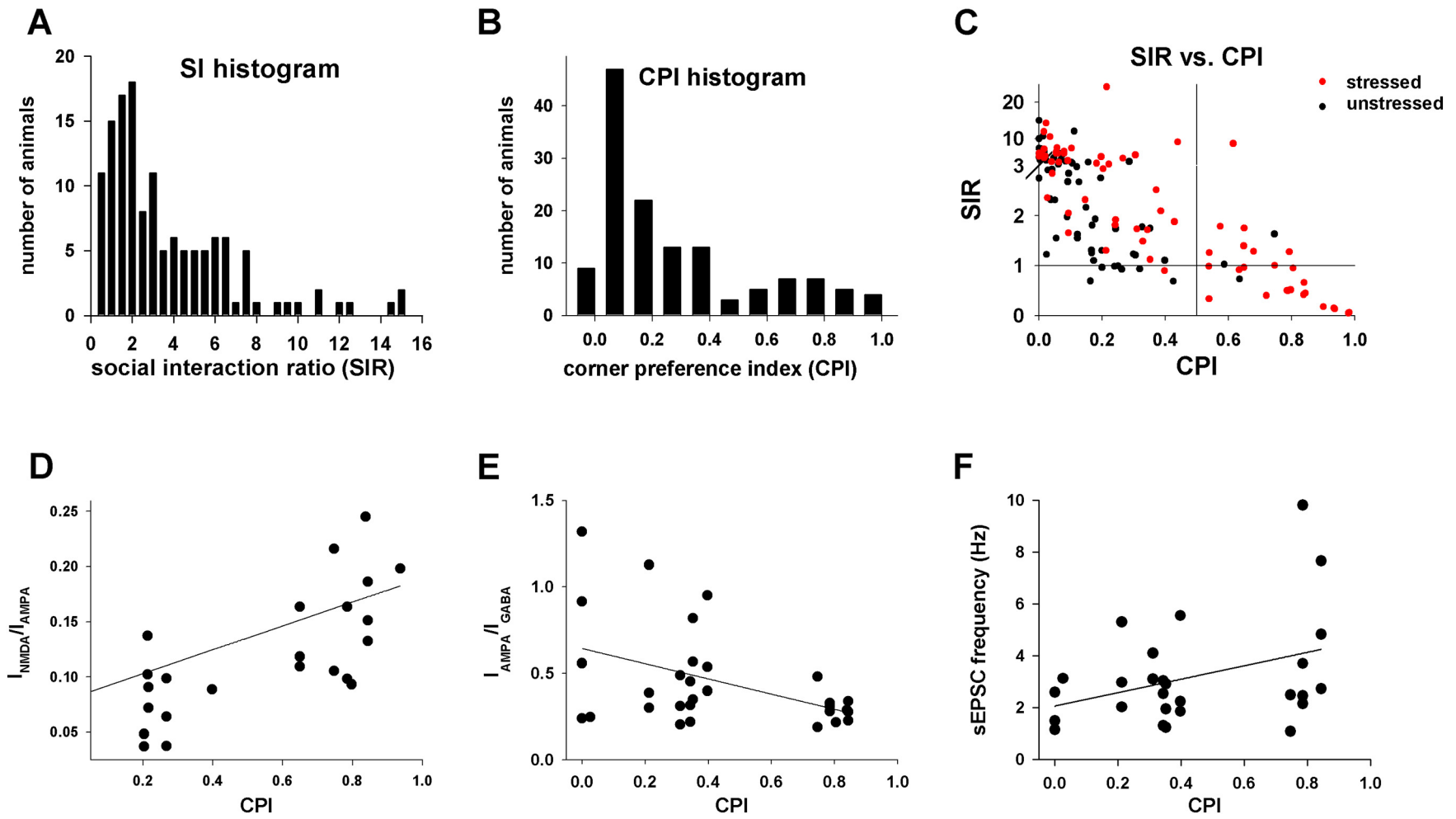

Fig. 6. Behavioral response to SD. Normalized distributions for Corner Preference Index **(CPI, A)**, Social Interaction ratio **(SIR, B)**. The distribution of SIR (Fig. 5A) does not display a clear separation between two different populations, whereas the distribution of CPI does (Fig. 5B), by setting a threshold at a value of CPI = 0.5. A graph correlating CPI with SIR (Fig. 5C, each dot represents an animal, black for unstressed, red for stressed) shows that the two criteria almost overlap. In fact, most of the population fills the upper left and lower right quadrants, being the amount of susceptible animals according to a SIR ≤1, S_{SIR} = 19%, while the same amount according to CPI, is S_{CPI} = 21%, and 87% of the animals fell into the same category (S or R) regardless of the criterion (CPI ≥ 0.5 or SIR ≤1). **(D) Correlation between I_{NMDA}/I_{AMPA} vs. CPI**. Each individual point represents one electrophysiological recording (n = 32 recordings from 10 animals). The line represents the linear regression of all experimental points, three of which have been left outside of the graph for better expansion. **(E) Correlation between I_{AMPA}/I_{GABA} vs. CPI**. Each individual point represents one electrophysiological recording (n = 30 recordings from 12 animals). The line represents the linear regression of all experimental points. **(D) Saturation level of evoked I_{GABA}** is higher in SD-susceptible WT animals vs. untreated WT. The effect of SD is absent in TG animals (third and fourth bars), consistent with the results in **(A)**. **(F)** Analogous to the previous figure, **correlation between sEPSC frequency** vs. CPI. Each individual point represents one electrophysiological recording (n = 27 recordings from 10 animals each graph). The lines represent the linear regression of all experimental points.

both), and TG (unstressed vs S, and unstressed vs. R, $p < 0.05$ both), indicating that the effect does not depend on IL-6 trans-signaling. Miniature IPSC *amplitude* (Fig. 5D), was significantly reduced in R animals (unstressed vs. R, $p < 0.05$), although both the pool of stressed as well as S animals displayed a tendency to a decreased amplitude (both $0.05 < p < 0.10$, Tukey test).

No effects of SD were detected on kinetic parameters (20–80% rise time, rt. and 50% half-width, hw) in either mEPSC or mIPSC WT or TG animals, except that R TG animals displayed a longer mIPSC half-width compared to controls and S animals (45 ± 4 ms for R vs. 30 ± 4 ms for control and 27 ± 5 ms for S, n = 10 each group). A summary of the effects of SD on synaptic activity is reported on Table 1.

Corner preference index correlates with electrophysiological parameters

While the Social Interaction Ratio (SIR) distribution failed to show clear-cut separation between populations (Fig. 6A), the distribution of the corner preference index (CPI) did show two clear populations with CPI = 0.5 as separation threshold (Fig. 6B). The two behavioral indicators were not independent as shown in Fig. 5C, representing the correlation between SIR and CPI. In fact, the majority (87%) of the animals categorized as S or R according to the criterion SIR < 1 or > 1, also displayed a CPI > 0.5 or < 0.5, respectively, suggesting that CPI may be a solid behavioral indicator, virtually equivalent to the SIR.

Interestingly, the ratio I_{NMDA}/I_{AMPA} CPI positively correlated with CPI (linear correlation coefficient $R = 0.35$, $p < 0.001$, n = 32 recordings from 10 animals, Fig. 6D). Opposite to the ratio I_{NMDA}/I_{AMPA}, the ratio I_{AMPA}/I_{GABA} correlated *negatively* with CPI (linear correlation coefficient $R = 0.49$, $p < 0.0001$, n = 30 recordings from 12 animals, Fig. 6E). These results represent an IL-6-dependent decrease in synaptic excitability associated with a SD-vulnerability. Similarly, sEPSC frequency positively correlated with CPI (Fig. 6F, coefficient of correlation $R = 0.45$, $p < 0.001$, n = 28 recordings from 10 animals).

DISCUSSION

We investigated for the first time the effect of SD and its IL-6 dependence on behavior and synaptic properties of the mPFC using a genetically modified C57BL/6 mouse strain in which central IL-6 trans-signaling was impaired. Our findings suggest that SD induces an IL-6 dependent plasticity of glutamatergic synapses in resilient animals, and a decrease in excitability in susceptible animals, besides other more complex effects. The present results suggest that a decrease in I_{NMDA}/I_{AMPA} and I_{AMPA}/I_{GABA} is the hallmark of SD induced synaptic plasticity in the mPFC. Interestingly, both specific changes detected for S animals (decrease in I_{AMPA}/I_{GABA}) and R animals (decrease in I_{NMDA}/I_{AMPA}) appear to be IL-6 dependent.

Effects of SD on behavioral response

The response to social interaction of unstressed (control) animals displayed a tendency of the (naïve) TG group to be less vulnerable compared to (naïve) WT, suggesting that basal levels of IL-6 trans-signaling may elevate the response to acute social stress. The data are in line with previous studies showing that increased levels of IL-6 are associated with sensitivity to SD after the first defeat (Hodes et al., 2014). The performance of mice subject to the *full* SD protocol showed that TG animals are *not* less susceptible to SD than WT animals, suggesting that SD may evoke a stressful response using molecular mechanisms other than CNS IL-6 trans-signaling. These results may not surprise, considering the existence of multiple alternative central pathways of stress, involving the hypothalamus–pituitary–adrenal (HPA) axis, the release of vasopressin and other stress-related peptides like other pro-inflammatory cytokines, as well monoamines, through cortical and/or sub-cortical IL-6-independent pathways (Atzori et al., 2016).

Effect of SD on synaptic functions

As error-sensor for working memory in executive function, the mPFC has long been proposed to be an area particularly susceptible to stress (Devilbiss et al., 2016). A basic question about the effects of stress is whether stress-resilience and/or stress-sensitivity are specifically associated with any peculiar form synaptic plasticity. Among many, two parameters are critical for synaptic function: 1) the proportion I_{NMDA}/I_{AMPA}, whose decrease parallels synaptic maturation and learning processes (Funahashi et al., 2013), and 2) the ratio I_{AMPA}/I_{GABA}, a crucial indicator of neuronal excitability. The decreased I_{NMDA}/I_{AMPA} detected specifically in WT resilient animals suggests that *adaptation* – or *resilience* – to stress is an *active* process, as previously suggested (Wilkinson et al., 2009), eliciting a specific change in mPFC glutamatergic circuitry. This interpretation is corroborated by the positive correlation between I_{NMDA}/I_{AMPA} and CPI, and by a negative correlation between I_{AMPA}/I_{GABA}. A decreased I_{AMPA}/I_{GABA} ratio is likely to cause a decrease in mPFC power. According to work from several groups (Kumar et al., 2014; Hultman et al., 2016), a decrease in mPFC power is a hallmark of stress-sensitive animals, consistent with the inverse correlation that we found between CPI and I_{AMPA}/I_{GABA}. Alterations in mPFC activation would eventually bring about a decrease in synchronization between limbic areas including amygdala, ventral tegmental area, and ventral striatum, leading, in turn, to depressive-like symptoms (Hultman et al., 2018).

A direct interaction between IL-6 and NMDAR (Qiu et al., 1998; Qiu and Gruol, 2003) may be at least partly responsible of this form of adaptation. On the contrary, the decrease in I_{AMPA}/I_{GABA} displayed specifically by SD-susceptible animals is consistent with the parallel increase displayed by GABAergic I/O saturation current, in agreement with an increase in inhibition caused by chronic stress (McKlveen et al., 2016; Jett et al., 2017), and with a loss of AMPAR induced by repeated restraint stress (Yuen et al., 2012; Wei et al., 2016b). Since in a previous study no appreciable baseline differences in either variable (I_{NMDA}/I_{AMPA} or I_{AMPA}/I_{GABA}) were detected between WT and TG animals (Cuevas-Olguin et al., 2017), our present results suggest

that a decrease in I_{NMDA}/I_{AMPA} and an increase in I_{GABA}/I_{AMPA} are a hallmark of SD induced synaptic plasticity in the mPFC.

Interestingly, both specific changes detected for S animals (decrease in I_{AMPA}/I_{GABA}) and R animals (decrease in I_{NMDA}/I_{AMPA}) appear to be IL-6 dependent. This observation highlights at once the importance of this cytokine in the occurrence of stress-induced plasticity, as well as its dual nature in the induction of mPFC plasticity. As a corollary, since IL-6 appears to be necessary for synaptic plasticity of both R and S animals – at least in the mPFC – it may prove difficult to use IL-6 cascade ligands to interfere specifically on the plasticity of specific stress-induced circuits.

The apparent discrepancy in the effect of stress on mIPSC frequency between our data and those by McKlveen and colleagues (McKlveen et al., 2016) may be due to the use of different stressors and/or species, as well as to possible differences in the actual (unknown) source of miniature events in the two preparations. The biological nature of the deficit suggests that a stress-induced difference in Cl^- driving force, as generated by a deficit in Cl^- transporter function is less likely (Maguire, 2014). Together, these results suggest that different types of synaptic plasticity are present in the mPFC of stress-susceptible vs. stress-resilient animals, possibly with different cellular mechanisms and timescales (Jackson and Moghaddam, 2006; Moghaddam, 2016). It is tempting to speculate that a causal relationship may connect a decreased I_{AMPA}/I_{GABA} and a diminished performance and function of the mPFC, consistent with pre-clinical and clinical data on depressed subjects, and with renewed attempts at targeting the main executive neurotransmitter system (glutamatergic and GABAergic) in the treatment of mood disorders (Sanacora et al., 2004).

In spite of the absence of SD effects on PPR of either excitatory or inhibitory synapses, analysis of miniature synaptic events showed that SD reduces the frequency of both mEPSCs (IL-6 dependent) and mIPSCs (IL-6 independent), with unchanged amplitude. A reduced frequency in SD mEPSC might be due to synaptic withdrawal and spine density decrease, as observed after sensory or restrain stress in the PFC (Soztutar et al., 2016), and other cortical areas (Bose et al., 2010). On the other hand, a decreased mIPSC frequency with unaltered amplitude in SD animals is consistent with a large body of literature reporting stress-induced deficit in GABAergic interneuron function (Tseng et al., 2008; Ganguly et al., 2015; Banasr et al., 2017; Ueno et al., 2017; Filipović et al., 2018), part of which has been hypothesized to be IL-6 dependent (Gumusoglu et al., 2017), and to an increased sensitivity to glutamatergic-induced seizures (Samland et al., 2003).

We speculate that the IL-6 dependent increase in sEPSC frequency, which we found to be specific for stress-susceptible (S) animals, accompanied by a non-specific amplitude decrease, might be caused by an *enhancement* in mPFC principal cells firing rate and their *reduced* synchronization. The corresponding firing enhancement, could be possibly caused by a disordered rearrangement of the mPFC local excitatory circuitry. In turn, this property might be a source of PFC decreased performance and behavioral ineffectiveness. Additionally, an increased sEPSC frequency in SD animals is consistent with enhanced mPFC excitatory – also possibly disorderly – activity, similarly detected in major depression (Zhang et al., 2016).

SD did not alter synaptic parameters of sIPSCs, but increased I_{GABA} saturation level in S animals, consistent with higher synchronicity of interneuronal ensembles, but in the absence of major physical rearrangement of the GABAergic interneuronal circuitry. Altogether, our results are integrated in the speculative (but testable) hypothesis summarized in the sketch of Fig. 7. An almost completely unaltered kinetics is consistent with a lack of major changes in synaptic receptors subunit composition. The only kinetic parameter changed by stress was measured in R TG animals, possibly due to a role of IL-6 in the stabilization of the turnover of one or more GABAR subunits (Garcia-Oscos et al., 2012).

Since in GFAP-sgp130Fc animals IL6 trans-signaling pathway was only modified in the brain and not in the periphery (Campbell et al., 2014), the synaptic effects of SD on the PFC, are not likely to be caused *exclusively* by changes in peripheral signaling of the immune system of the mice. However, we cannot exclude that the synaptic effects of SD on the PFC are caused indirectly, by alterations in peripheral function, such as social stressor-induced changes in intestinal immunomodulation, which was also found to be IL-6 dependent (Bailey et al., 2011; Burokas et al., 2017; Szyszkowicz et al., 2017). This possibility is further supported by a stress-induced weakening of the blood brain barrier allowing peripheral IL-6 to reach the CNS (Menard et al., 2017), and by the occurrence of anxiety symptoms following SD-promoted splenic activation (McKim et al., 2016). A correlation between stress, gut microbiota, and IL-6 mediated central maladaptive plasticity should thus not be overlooked (Zhang et al., 2017). Besides the relevance of IL-6-dependent mechanisms in the PFC, a further possible explanation for the ineffectiveness of SD to induce synaptic changes in TG animals could be the presence of IL-6-dependent effects in sub-cortical areas, particularly in the ventral striatum (N. Accumbens), known to interfere in reward related tasks (Treadway et al., 2017).

The cellular mechanisms through which IL-6 affects synaptic function are yet incompletely understood. We proposed in earlier work that IL-6 may be *acutely* modulating translational or post-translational intracellular receptor trafficking (Garcia-Oscos et al., 2012), notion supported by the modulation of membrane receptor function after IL-6 elevation following lipopolysaccharide injections (Chugh et al., 2013), and by interactions of this cytokine with eukaryotic initiation factor 4, a crucial protein for ribosomal function (Melemedjian et al., 2010). Our present data suggest that presynaptic, structural, and anatomical factors may embody the core of *chronic* social stress synaptic alterations, following a period of acute stress, in which – on the contrary – postsynaptic alterations may be induced in a relatively short time-scale, as corroborated by the effectiveness of intracellular tyrosine kinase inhibitors in blocking IL-6-induced synaptic plasticity (Tancredi et al., 2000).

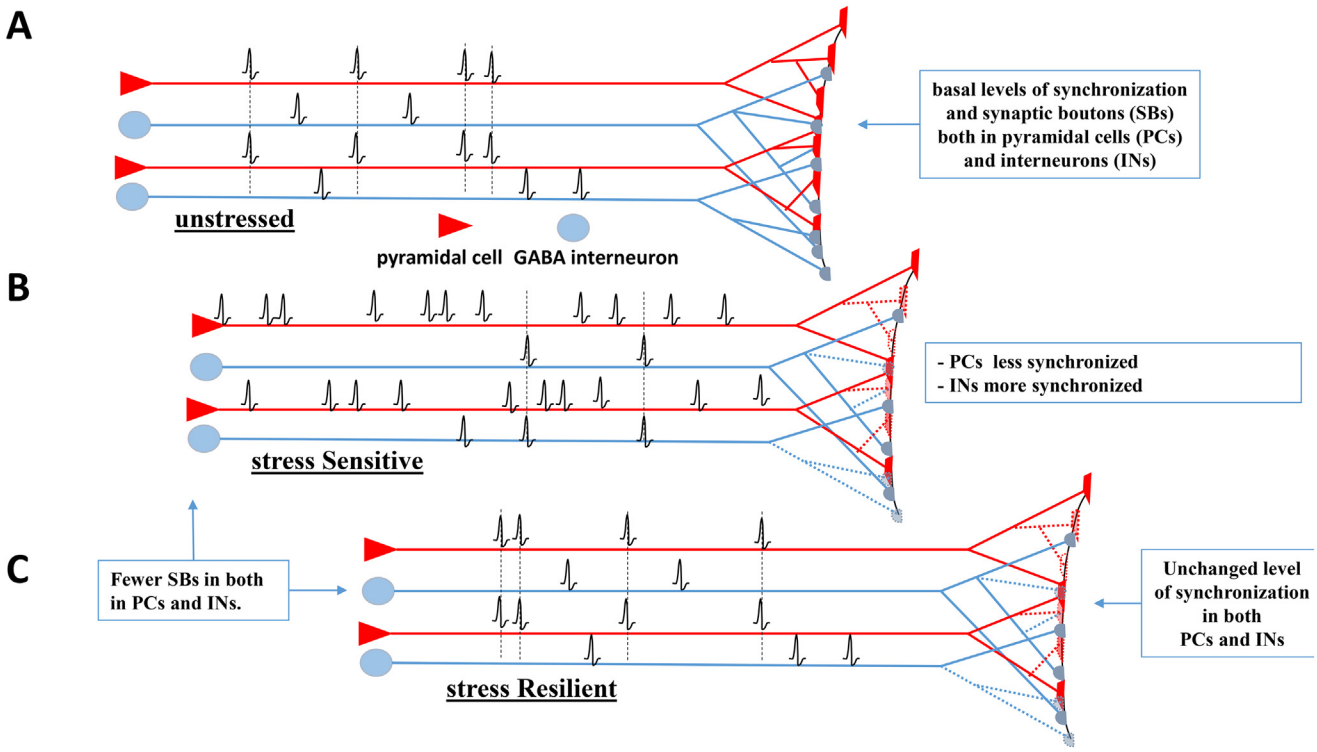

Fig. 7. Representation of the possible effects of SD on mPFC activity. Legend: red, triangular, cells represent principal pyramidal neurons of the mPFC, blue circles represent inhibitory GABAergic mPFC interneurons, each one with a related firing pattern. Red and blue spots on the right represent corresponding synapses. **(A) Unstressed animals** possess a moderate firing frequency with a basal degree of synchronicity and synaptic connectivity, represented by the density of red and blue spots on the right. **(B) Stress-Sensitive** animals present fewer synapses (dashed lines) and a higher firing frequency. Synchronization is decreased in principal cell but decreased in inhibitory interneurons. **(C) Stress-Resilient animals** are able to maintain baseline synchronization but have a similar decrease in both excitatory and inhibitory synaptic connectivity.

Our data corroborate the hypothesis that chronic distress leads to considerable changes in synaptic function, and suggest that 1) the mPFC undergoes major rearrangements after SD, 2) a great extent of the SD-induced synaptic changes elicited in the mPFC of the intact animal is dependent on IL-6 trans-signaling, 3) susceptible (S) and resilient (R) animals undergo different types of SD-induced synaptic changes, and 4) some of the changes associated with SD-sensitivity and SD-resilience in the mPFC are specifically dependent on IL-6 trans-signaling. IL-6 trans-signaling appears thus to be a critical component in stress-induced re-shaping of PFC synaptic connectivity.

While numerous SD-induced differences in synaptic plasticity between WT and TG animals indicate that IL-6 is a crucial factor in synaptic rearrangement elicited by stress in the mPFC, on the other hand, the sensitivity of TG animals to SD indicates the existence of stress mechanisms independent from central IL-6 signaling. Early neurodevelopmental alterations in synaptic transmission of TG animals may explain their unchanged sensitivity to SD (Cuevas-Olguin et al., 2017). Alternatively, other stress-related pathways like direct connections from the amygdala to the motor cortices, to other pre-motor areas, or with the PFC itself might be responsible for eliciting the fear response through IL-6 independent mechanisms.

Further studies will be necessary to: 1) corroborate whether stress produces opposite effects on neuronal firing synchronicity for principal cells vs. GABAergic interneurons in stress-susceptible animals, 2) separate the specific effects of IL-6 on different types of GABAergic interneurons, 3) determine the specific intracellular mechanisms triggered by stress through IL-6, and 4) understand IL-6 dependent synaptic and neuronal mechanisms in brain areas other than the mPFC, such as the amygdala (Jasnow et al., 2005), hippocampus (Olde Engberink et al., 2017), and the ventral tegmental area (Fanous et al., 2010).

ACKNOWLEDGMENTS

This study was performed in part with funds from CONACyT to MA (CB 2013-221653). Dr. Rose-John is funded by grants from the Deutsche Forschungsgemeinschaft, Bonn, Germany (SFB654, project C5; SFB841, project C1; SFB877, project A1) and by the Cluster of Excellence “Inflammation at Interfaces.” Dr. Rose-John is an inventor on the patent describing the function of sgp130Fc. He is also a shareholder of the CONARIS Research Institute (Kiel, Germany), which is commercially developing sgp130Fc as a therapy for inflammatory diseases. All other authors reported no biomedical financial interests or potential conflicts of interest. We would like to thank Dr. Juan

Francisco Lopez Rodriguez and all personnel at UASLP Faculty of Medicine animal facility for animal breeding, preparation, and maintenance.

REFERENCES

Agorastos Agorastos, Pervanidou Panagiota, Chrousos George P, Baker Dewleen G. (2019) Developmental trajectories of early life stress and trauma: a narrative review on neurobiological aspects beyond stress system dysregulation. Front Psych 10:118.

Arnsten Amy FT. (2009) "Stress signalling pathways that impair prefrontal cortex structure and function." *Nature Reviews*. Neuroscience 10 (6):410-422.

Atzori Marco, Garcia-Oscos Francisco, Mendez JA Jose Alfredo. (2012) Role of IL-6 in the etiology of hyperexcitable neuropsychiatric conditions: experimental evidence and therapeutic implications. Future Med Chem 4(17):2177-2192.

Atzori Marco, Cuevas-Olguin Roberto, Esquivel-Rendon Eric, Garcia-Oscos Francisco, Salgado-Delgado Roberto C, Saderi Nadia, Miranda-Morales Marcela, Treviño Mario, Pineda Juan C, Salgado Humberto. (2016) Locus ceruleus norepinephrine release: a central regulator of CNS spatio-temporal activation? Frontiers in Synaptic Neuroscience 8.

Bailey Michael T, Dowd Scot E, Galley Jeffrey D, Hufnagle Amy R, Allen Rebecca G, Lyte Mark. (2011) Exposure to a social stressor alters the structure of the intestinal microbiota: implications for stressor-induced immunomodulation. Brain Behav Immun 25(3):397-407.

Banasr, Mounira, Ashley Lepack, Corey Fee, Vanja Duric, Jaime Maldonado-Aviles, Ralph DiLeone, Etienne Sibille, Ronald S. Duman, and Gerard Sanacora. 2017. "Characterization of GABAergic marker expression in the chronic unpredictable stress model of depression." *Chronic Stress (Thousand Oaks, Calif.)* 1.

Bose M, Muñoz-Llancao P, Roychowdhury S, Nichols JAA, Jakkamsetti V, Porter B, Byrapureddy R, Salgado H, Kilgard MPP, Aboitiz F, Dagnino-Subiabre A, Atzori M, Munoz-Llancao P, Roychowdhury S, Nichols JAA, Jakkamsetti V, Porter B, Byrapureddy R, Salgado H, Kilgard MPP, Aboitiz F, Dagnino-Subiabre A, Atzori M. (2010) Effect of the environment on the dendritic morphology of the rat auditory cortex. Synapse (New York, N Y) 64(2):97-110.

Burokas Aurelijus, Arboleya Silvia, Moloney Rachel D, Peterson Veronica L, Murphy Kiera, Clarke Gerard, Stanton Catherine, Dinan Timothy G, Cryan John F. (2017) Targeting the microbiota–gut–brain axis: prebiotics have anxiolytic and antidepressant-like effects and reverse the impact of chronic stress in mice. Biol Psychiatry 82 (7):472-487.

Campbell IL, Erta M, Lim SL, Frausto R, May U, Rose-John S, Scheller J, Hidalgo J. (2014) Trans-signaling is a dominant mechanism for the pathogenic actions of Interleukin-6 in the brain. The Journal Of Neuroscience: The Official Journal Of The Society For Neuroscience 34(7):2503-2513.

Chugh Deepti, Nilsson Per, Afjei Seyedeh-Atiyeh, Bakochi Anahita, Ekdahl Christine T. (2013) Brain inflammation induces post-synaptic changes during early synapse formation in adult-born hippocampal neurons. Exp Neurol 250:176-188.

Cuevas-Olguin Roberto, Esquivel-Rendon Eric, Vargas-Mireles Jorge, Garcia-Oscos Francisco, Miranda-Morales Marcela, Salgado Humberto, Rose-John Stefan, Atzori Marco. (2017) Interleukin 6 trans-signaling regulates basal synaptic transmission and sensitivity to pentylenetetrazole-induced seizures in mice. Synapse 71(9)e21984.

Cusick Matthew F, Libbey Jane E, Doty Daniel J, DePaula-Silva Ana Beatriz, Fujinami Robert S. (2017) The role of peripheral interleukin-6 in the development of acute seizures following virus encephalitis. J Neurovirol 23(5):696-703.

Dantzer Robert, O'Connor Jason C, Freund Gregory G, Johnson Rodney W, Kelley Keith W. (2008) "From inflammation to sickness and depression: when the immune system subjugates the brain." *Nature Reviews*. Neuroscience 9(1):46-56.

Devilbiss, David M., Robert C. Spencer, and Craig W. Berridge. 2016. "Stress degrades prefrontal cortex neuronal coding of goal-directed behavior." *Cerebral Cortex* 27(5):bhw140.

Dowlati Yekta, Herrmann Nathan, Swardfager Walter, Liu Helena, Sham Lauren, Reim Elyse K, Lanctôt Krista L. (2010) A meta-analysis of cytokines in major depression. Biol Psychiatry 67(5):446-457.

Dufour F, Liu QY, Gusev P, Alkon D, Atzori M. (2006) Cholesterol-enriched diet affects spatial learning and synaptic function in hippocampal synapses. Brain Res 1103(1).

Engberink Olde, Anneke Ruben Hernandez, de Graan Pierre, Gruol Donna L. (2017) Rapamycin-sensitive late-LTP is enhanced in the hippocampus of IL-6 transgenic mice. Neuroscience 367:200-210.

Fanous S, Hammer RP, Nikulina EM. (2010) Short- and long-term effects of intermittent social defeat stress on brain-derived neurotrophic factor expression in mesocorticolimbic brain regions. Neuroscience 167(3):598-607.

Ferguson Brielle R, Gao Wen-Jun. (2018) PV interneurons: critical regulators of E/I balance for prefrontal cortex-dependent behavior and psychiatric disorders. Frontiers in Neural Circuits 12:37.

Filipović Dragana, Stanisavljević Andrijana, Jasnić Nebojša, Bernardi Rick E, Inta Dragos, Perić Ivana, Gass Peter. (2018) Chronic treatment with fluoxetine or clozapine of socially isolated rats prevents subsector-specific reduction of parvalbumin immunoreactive cells in the Hippocampus. Neuroscience 371:384-394.

Funahashi Rie, Maruyama Takuro, Yoshimura Yumiko, Komatsu Yukio. (2013) Silent synapses persist into adulthood in layer 2/3 pyramidal neurons of visual cortex in dark-reared mice. J Neurophysiol 109 (8):2064-2076.

Ganguly Prabarna, Holland Freedom H, Brenhouse Heather C. (2015) Functional uncoupling NMDAR NR2A subunit from PSD-95 in the prefrontal cortex: effects on behavioral dysfunction and parvalbumin loss after early-life stress. Neuropsychopharmacology 40(12):2666-2675.

Garbers Christoph, Heink Sylvia, Korn Thomas, Rose-John Stefan. (2018) Interleukin-6: designing specific therapeutics for a complex cytokine. Nat Rev Drug Discov 17:395-412.

Garcia-Oscos F, Salgado H, Hall S, Thomas F, Farmer GEE, Bermeo J, Galindo LCC, Ramirez RDD, D'Mello S, Rose-John S, Atzori M. (2012) The stress-induced cytokine interleukin-6 decreases the inhibition/excitation ratio in the rat temporal cortex via trans-signaling. Biol Psychiatry 71(7):574-582.

Garcia-Oscos F, Peña D, Housini M, Cheng D, Lopez D, Borland MSS, Salgado-Delgado R, Salgado-Burgos H, D'Mello S, Kilgard MPP, Rose-John S, Atzori M, Salgado H, D'Mello S, Kilgard MPP, Rose-John S, Atzori M. (2014) Vagal nerve stimulation blocks interleukin 6-dependent synaptic hyperexcitability induced by lipopolysaccharide-induced acute stress in the rodent prefrontal cortex. Brain: Behavior and Immunity in press, 2014.

Gimeno D, Kivimäki M, Brunner EJ, Elovainio M, De Vogli R, Steptoe A, Kumari M, Lowe GDO, Rumley A, Marmot MG, Ferrie JE. (2009) Associations of C-reactive protein and interleukin-6 with cognitive symptoms of depression: 12-year follow-up of the Whitehall II study. Psychol Med 39(03):413.

Golden Sam A, Covington Herbert E, Berton Olivier, Russo Scott J. (2011) A standardized protocol for repeated social defeat stress in mice. Nat Protoc 6(8):1183-1191.

Gumusoglu Serena B, Fine Rebecca S, Murray Samuel J, Bittle Jada L, Stevens Hanna E. (2017) The role of IL-6 in neurodevelopment after prenatal stress. Brain Behav Immun 65:274-283.

Hanse Eric, Seth Henrik, Riebe Ilse. (2013) AMPA-silent synapses in brain development and pathology. Nat Rev Neurosci 14(12):839-850.

Heese Klaus. (2017) Functional repertoire of interleukin-6 in the central nervous system — a review. Restor Neurol Neurosci 35(6):693-701.

Hernandez Ruben V, Puro Alana C, Manos Jessica C, Huitron-Resendiz Salvador, Reyes Kenneth C, Liu Kevin, Vo Khanh, Roberts Amanda J, Gruol Donna L. (2016) Transgenic mice with increased astrocyte expression of IL-6 show altered effects of acute ethanol on synaptic function. Neuropharmacology 103:27-43.

Hinkle LE. (1987) Stress and disease: the concept after 50 years. Soc Sci Med 25(6):561-566.

Hodes Georgia E, Pfau Madeline L, Leboeuf Marylene, Golden Sam A, Christoffel Daniel J, Bregman Dana, Rebusi Nicole, Heshmati Mitra, Aleyasin Hossein, Warren Brandon L, Labonté Benoit, Horn Sarah,

Lapidus Kyle A, Stelzhammer Viktoria, Wong Erik HF, Bahn Sabine, Krishnan Vaishnav, Bolaños-Guzman Carlos A, Murrough James W, Merad Miriam, Russo Scott J. (2014) Individual differences in the peripheral immune system promote resilience versus susceptibility to social stress. Proc Natl Acad Sci 111(45):16136-16141.

Holmes Andrew, Wellman Cara L. (2009) Stress-induced prefrontal reorganization and executive dysfunction in rodents. Neurosci Biobehav Rev 33(6):773-783.

Hultman Rainbo, Mague Stephen D, Li Qiang, Katz Brittany M, Michel Nadine, Lin Lizhen, Wang Joyce, David Lisa K, Blount Cameron, Chandy Rithi, Carlson David, Ulrich Kyle, Carin Lawrence, Dunson David, Kumar Sunil, Deisseroth Karl, Moore Scott D, Dzirasa Kafui. (2016) Dysregulation of prefrontal cortex-mediated slow-evolving limbic dynamics drives stress-induced emotional pathology. Neuron 91(2):439-452.

Hultman, Rainbo, Kyle Ulrich, Benjamin D. Sachs, Cameron Blount, David E. Carlson, Nkemdilim Ndubuizu, Rosemary C. Bagot, Eric M. Parise, Mai-Anh T. Vu, Neil M. Gallagher, Joyce Wang, Alcino J. Silva, Karl Deisseroth, Stephen D. Mague, Marc G. Caron, Eric J. Nestler, Lawrence Carin, and Kafui Dzirasa. 2018. “Brain-wide electrical spatiotemporal dynamics encode depression vulnerability.” *Cell* 173(1):166–180.e14.

Jackson Mark E, Moghaddam Bita. (2006) Distinct patterns of plasticity in prefrontal cortex neurons that encode slow and fast responses to stress. Eur J Neurosci 24(6):1702-1710.

Jacoby Anne Sophie, Munkholm Klaus, Vinberg Maj, Pedersen Bente Klarlund, Kessing Lars Vedel. (2016) Cytokines, brain-derived neurotrophic factor and C-reactive protein in bipolar I disorder — results from a prospective study. J Affect Disord 197:167-174.

Jansen R, Penninx BWJH, Madar V, Xia K, Milaneschi Y, Hottenga JJ, Hammerschlag AR, Beekman A, van der Wee N, Smit JH, Brooks AI, Tischfield J, Posthuma D, Schoevers R, van Grootheest G, Willemsen G, de Geus EJ, Boomsma DI, Wright FA, Zou F, Sun W, Sullivan PF. (2016) Gene expression in major depressive disorder. Mol Psychiatry 21(3):339-347.

Jasnow Aaron M, Shi Chanjun, Israel Jeris E, Davis Michael, Huhman Kim L. (2005) Memory of social defeat is facilitated by CAMP response element-binding protein overexpression in the amygdala. Behav Neurosci 119(4):1125-1130.

Jett Julianne D, Bulin Sarah E, Hatherall Lauren C, McCartney Carlie M, Morilak David A. (2017) Deficits in cognitive flexibility induced by chronic unpredictable stress are associated with impaired glutamate neurotransmission in the rat medial prefrontal cortex. Neuroscience 346:284-297.

Kawasaki Y, Zhang L, Cheng JK, Ji RR. (2008) Cytokine mechanisms of central sensitization: distinct and overlapping role of interleukin-1beta, interleukin-6, and tumor necrosis factor-alpha in regulating synaptic and neuronal activity in the superficial spinal cord. The Journal Of Neuroscience: The Official Journal Of The Society For Neuroscience 28(20):5189-5194.

Kim J, Alger BE. (2001) Random response fluctuations lead to spurious paired-pulse facilitation. The Journal Of Neuroscience: The Official Journal Of The Society For Neuroscience 21(24):9608-9618.

Kumar Sunil, Hultman Rainbo, Hughes Dalton, Michel Nadine, Katz Brittany M, Dzirasa Kafui. (2014) Prefrontal cortex reactivity underlies trait vulnerability to chronic social defeat stress. Nat Commun 5(1):4537.

Lee Eunee, Lee Jiseok, Kim Eunjoon. (2017) Excitation/inhibition imbalance in animal models of autism spectrum disorders. Biol Psychiatry 81(10):838-847.

Li Xiaoning, Chen Weiqiang, Sheng Jiangtao, Cao Deliang, Wang Wanchun. (2014) Interleukin-6 inhibits voltage-gated sodium channel activity of cultured rat spinal cord neurons. Acta Neuropsychiatrica 26(03):170-177.

Liao Dezhi, Hessler Neal A, Malinow Roberto. (1995) Activation of postsynaptically silent synapses during pairing-induced LTP in CA1 region of hippocampal slice. Nature 375(6530):400-404.

Lin Kuei-Ying, Cherng Chianfang G, Yang Fu-Rong, Lin Li-Ching, Lu Ru-Band, Lung Yu. (2011) Memantine abolishes the formation of cocaine-induced conditioned place preference possibly via its IL-6-modulating effect in medial prefrontal cortex. Behav Brain Res 220 (1):126-131.

Luque-García Aina, Teruel-Martí Vicent, Martínez-Bellver Sergio, Adell Albert, Cervera-Ferri Ana, Martínez-Ricós Joana. (2018) Neural oscillations in the infralimbic cortex after electrical stimulation of the amygdala. Relevance to acute stress processing. J Comp Neurol 526(8):1403-1416.

Macht Victoria A, Reagan Lawrence P. (2017) Chronic stress from adolescence to aging in the prefrontal cortex: a neuroimmune perspective. Front Neuroendocrinol 49:31-42.

Maffei A, Nelson SB, Turrigiano GG. (2004) Selective reconfiguration of layer 4 visual cortical circuitry by visual deprivation. Nat.Neurosci 7 (12):1353-1359.

Maguire Jamie. (2014) Stress-induced plasticity of GABAergic inhibition. Front Cell Neurosci 8:157.

McKim Daniel B, Patterson Jenna M, Wohleb Eric S, Jarrett Brant L, Reader Brenda F, Godbout Jonathan P, Sheridan John F. (2016) Sympathetic release of splenic monocytes promotes recurring anxiety following repeated social defeat. Biol Psychiatry 79(10):803-813.

McKlveen Jessica M, Morano Rachel L, Fitzgerald Maureen, Zoubovsky Sandra, Cassella Sarah N, Scheimann Jessie R, Ghosal Sriparna, Mahbod Parinaz, Packard Benjamin A, Myers Brent, Baccei Mark L, Herman James P. (2016) Chronic stress increases prefrontal inhibition: a mechanism for stress-induced prefrontal dysfunction. Biol Psychiatry 80(10):754-764.

Melemedjian Ohannes K, Asiedu Marina N, Tillu Dipti V, Peebles Katherine A, Yan Jin, Ertz Natalie, Dussor Gregory O, Price Theodore J. (2010) IL-6- and NGF-induced rapid control of protein synthesis and nociceptive plasticity via convergent signaling to the EIF4F complex. J Neurosci 30(45):15113-15123.

Menard Caroline, Pfau Madeline L, Hodes Georgia E, Kana Veronika, Wang Victoria X, Bouchard Sylvain, Takahashi Aki, Flanigan Meghan E, Aleyasin Hossein, LeClair Katherine B, Janssen William G, Labonté Benoit, Parise Eric M, Lorsch Zachary S, Golden Sam A, Heshmati Mitra, Tamminga Carol, Turecki Gustavo, Campbell Matthew, Fayad Zahi A, Tang Cheuk Ying, Merad Miriam, Scott J. Russo. . (2017) Social stress induces neurovascular pathology promoting depression. Nat Neurosci 20(12):1752-1760.

Milenkovic Vladimir M, Stanton Evan H, Nothdurfter Caroline, Rupprecht Rainer, Wetzel Christian H. (2019) The role of chemokines in the pathophysiology of major depressive disorder. Int J Mol Sci 20(9):2283.

Moga DE, Shapiro ML, Morrison JH. (2006) Bidirectional redistribution of AMPA but not NMDA receptors after perforant path simulation in the adult rat hippocampus in vivo. Hippocampus 16(11):990-1003.

Moghaddam Bita. (2016) The complicated relationship of stress and prefrontal cortex. Biol Psychiatry 80(10):728-729.

Potvin Stéphane Stephane, Stip Emmanuel, Sepehry Amir A, Gendron Alain, Bah Ramatoulaye, Kouassi Edouard. (2008) Inflammatory cytokine alterations in schizophrenia: a systematic quantitative review. Biol Psychiatry 63(8):801-808.

Qi Chu-Chu, Wang Qing-Jun, Ma Xue-zhu, Chen Hai-Chao, Gao Li-Ping, Yin Jie, Jing Yu-Hong. (2018) Interaction of basolateral amygdala, ventral hippocampus and medial prefrontal cortex regulates the consolidation and extinction of social fear. Behav Brain Funct 14(1):7.

Qiu Zhihua, Gruol Donna L. (2003) Interleukin-6, beta-amyloid peptide and NMDA interactions in rat cortical neurons. J Neuroimmunol 139(1–2):51-57.

Qiu Z, Sweeney DD, Netzeband JG, Gruol DL. (1998) Chronic interleukin-6 alters NMDA receptor-mediated membrane responses and enhances neurotoxicity in developing CNS neurons. J Neurosci 18(24):10445-10456.

Ramirez Karol, Sheridan John F. (2016) Antidepressant imipramine diminishes stress-induced inflammation in the periphery and central nervous system and related anxiety- and depressive- like behaviors. Brain Behav Immun 57:293-303.

Rose-John S. (2012) IL-6 trans-signaling via the soluble IL-6 receptor: importance for the pro-inflammatory activities of IL-6. Int J Biol Sci 8(9):1237-1247.

Rothaug Michelle, Becker-Pauly Christoph, Rose-John Stefan. (2016) The role of interleukin-6 signaling in nervous tissue. Biochimica et

Biophysica Acta (BBA) - Molecular Cell Research 1863(6):1218-1227.
Roychowdhury Swagata, Amy AN, Zwierzchowski N, Francisco Garcia-Oscos, Olguin RC Roberto Cuevas, Delgado Roberto Salgado RS, Atzori Marco. (2014) Layer- and area-specificity of the adrenergic modulation of synaptic transmission in the rat neocortex. Neurochem Res 39(12):2377-2384.
Samland H, Huitron-Resendiz S, Masliah E, Criado J, Henriksen SJ, Campbell IL. (2003) Profound increase in sensitivity to glutamatergic- but not cholinergic agonist-induced seizures in transgenic mice with astrocyte production of IL-6. J Neurosci Res 73(2):176-187.
Sanacora G, Gueorguieva R, Epperson CN, Wu YT, Appel M, Rothman DL, Krystal JH, Mason GF. (2004) Subtype-specific alterations of gamma-aminobutyric acid and glutamate in patients with major depression. Arch Gen Psychiatry 61(7):705-713.
Scheller J, Chalaris A, Schmidt-Arras D, Rose-John S. (2011) The pro- and anti-inflammatory properties of the cytokine interleukin-6. Biochim Biophys Acta 1813(5):878-888.
Selye H. (1976) Forty years of stress research: principal remaining problems and misconceptions. Can Med Assoc J 115(1):53-56.
Slavich George M, Irwin Michael R. (2014) From stress to inflammation and major depressive disorder: a social signal transduction theory of depression. Psychol Bull 140(3):774-815.
Soztutar Erdem, Colak Ertugrul, Ulupinar Emel. (2016) Gender- and anxiety level-dependent effects of perinatal stress exposure on medial prefrontal cortex. Exp Neurol 275:274-284.
Szyszkowicz Joanna Kasia, Wong Alex, Anisman Hymie, Merali Zul, Audet Marie-Claude. (2017) Implications of the gut microbiota in vulnerability to the social avoidance effects of chronic social defeat in male mice. Brain Behav Immun 66:45-55.
Tancredi V, D'Antuono M, Cafè C, Giovedì S, Buè MC, D'Arcangelo G, Onofri F, Benfenati F. (2000) The inhibitory effects of Interleukin-6 on synaptic plasticity in the rat hippocampus are associated with an inhibition of mitogen-activated protein kinase ERK. J Neurochem 75(2):634-643.
Tang Zhen, Ye Gang, Chen Xinyun, Pan Mingzhi, Jialin Fu, Tian Fu, Liu Qichun, Gao Zhenyong, Baldwin David S, Hou Ruihua. (2018) Peripheral proinflammatory cytokines in Chinese patients with generalised anxiety disorder. J Affect Disord 225:593-598.
Tatti Roberta, Haley Melissa S, Swanson Olivia K, Tselha Tenzin, Maffei Arianna. (2017) Neurophysiology and regulation of the balance between excitation and inhibition in neocortical circuits. Biol Psychiatry 81(10):821-831.
Thomas Mark J, Beurrier Corinne, Bonci Antonello, Malenka Robert C. (2001) Long-term depression in the nucleus accumbens: a neural correlate of behavioral sensitization to cocaine. Nat Neurosci 4 (12):1217-1223.
Treadway Michael T, Admon Roee, Arulpragasam Amanda R, Mehta Malavika, Douglas Samuel, Vitaliano Gordana, Olson David P, Cooper Jessica A, Pizzagalli Diego A. (2017) Association between interleukin-6 and striatal prediction-error signals following acute stress in healthy female participants. Biol Psychiatry 82(8):570-577.
Tseng KY, Lewis BL, Hashimoto T, Sesack SR, Kloc M, Lewis DA, O'Donnell P. (2008) A neonatal ventral hippocampal lesion causes functional deficits in adult prefrontal cortical interneurons. The Journal Of Neuroscience: The Official Journal Of The Society For Neuroscience 28(48):12691-12699.
Ueno Hiroshi, Suemitsu Shunsuke, Murakami Shinji, Kitamura Naoya, Wani Kenta, Okamoto Motoi, Matsumoto Yosuke, Ishihara Takeshi. (2017) Region-specific impairments in parvalbumin interneurons in social isolation-reared mice. Neuroscience 359:196-208.
Vezzani, Annamaria and Barbara Viviani. 2015. “Neuromodulatory properties of inflammatory cytokines and their impact on neuronal excitability.” *Neuropharmacology* 96(Pt A):70–82.
Wang Qiong, Shao Feng, Wang Weiwen. (2018) Region-dependent alterations in cognitive function and ERK1/2 signaling in the PFC in rats after social defeat stress. Neural Plast 2018:1-11.
Wei Hongen, Ma Yuehong, Liu Jianrong, Ding Caiyun, Jin Guorong, Wang Yi, Hu Fengyun, Li Yu. (2016) Inhibition of IL-6 trans-signaling in the brain increases sociability in the BTBR mouse model of autism. Biochimica et Biophysica Acta (BBA) - Molecular Basis of Disease 1862(10):1918-1925.
Wei J, Xiong Z, Lee JB, Cheng J, Duffney LJ, Matas E, Yan Z. (2016) Histone modification of Nedd4 ubiquitin ligase controls the loss of AMPA receptors and cognitive impairment induced by repeated stress. J Neurosci 36(7):2119-2130.
Wilkinson MB, Xiao G, Kumar A, LaPlant Q, Renthal W, Sikder D, Kodadek TJ, Nestler EJ. (2009) Imipramine treatment and resiliency exhibit similar chromatin regulation in the mouse nucleus accumbens in depression models. J Neurosci 29(24):7820-7832.
Wolf J, Rose-John S, Garbers C. (2014) Interleukin-6 and its receptors: a highly regulated and dynamic system. Cytokine 70:11-20.
Wu, G., R. Malinow, and H. T. Cline. 1996. “Maturation of a central glutamatergic synapse.” *Science (New York, N.Y.)* 274(5289):972–76.
Xia Wei, Peng Guo-yi, Sheng Jiang-tao, Zhu Fang-fang, Guo Jing-fang, Chen Wei-qiang. (2015) Neuroprotective effect of Interleukin-6 regulation of voltage-gated Na+ channels of cortical neurons is time- and dose-dependent. Neural Regen Res 10(4):610.
Yang Chun, Shirayama Yukihiko, Zhang Ji-Chun, Ren Qian, Hashimoto Kenji. (2015) Peripheral interleukin-6 promotes resilience versus susceptibility to inescapable electric stress. Acta Neuropsychiatrica 27(5):312-316.
Yang Jian-Jun, Wang Nan, Yang Chun, Shi Jin-Yun, Yu Hai-Ying, Hashimoto Kenji. (2015) Serum interleukin-6 is a predictive biomarker for ketamine's antidepressant effect in treatment-resistant patients with major depression. Biol Psychiatry 77(3):e19-e20.
Yuen Eunice Y, Wei Jing, Liu Wenhua, Zhong Ping, Li Xiangning, Yan Zhen. (2012) Repeated stress causes cognitive impairment by suppressing glutamate receptor expression and function in prefrontal cortex. Neuron 73(5):962-977.
Zhang Xiaoliu, Tang Yingying, Maletic-Savatic Mirjana, Sheng Jianhua, Zhang Xuanhong, Zhu Yajing, Zhang Tianhong, Wang Junjie, Tong Shanbao, Wang Jijun, Li Yao. (2016) Altered neuronal spontaneous activity correlates with glutamate concentration in medial prefrontal cortex of major depressed females: an FMRI-MRS study. J Affect Disord 201:153-161.
Zhang J-c, Yao W, Dong C, Yang C, Ren Q, Ma M, Hashimoto K. (2017) Blockade of Interleukin-6 receptor in the periphery promotes rapid and sustained antidepressant actions: A possible role of gut–microbiota–brain Axis. Transl Psychiatry 7(5)e1138.

(Received 5 March 2019, Accepted 1 July 2019)
(Available online 10 July 2019)